THESIS

A STRAINED RELATIONSHIP: THE EFFECTS OF PRUNING TREATMENTS ON WIND-INDUCED BENDING MOMENTS OF COLORADO BLUE SPRUCE (*PICEA PUNGENS*)

Submitted by

David James Leinbach

Department of Horticulture and Landscape Architecture

In partial fulfillment of the requirements

For the Degree of Master of Science

Colorado State University

Fort Collins, Colorado

Spring 2025

Master's Committee:

Advisor: Daniel C. Burcham

Yanlin Guo
Anthony Koski

ABSTRACT

A STRAINED RELATIONSHIP: THE EFFECTS OF PRUNING TREATMENTS ON WIND-INDUCED BENDING MOMENTS OF COLORADO BLUE SPRUCE (*PICEA PUNGENS*)

Wind and trees often have a strained relationship; and severe wind events can lead to tree loss, personal injury, and costly litigation. Pruning is a common practice used by arborists to mitigate the risk of tree failure by selectively removing parts of a tree crown exposed to the wind, but there are few existing studies examining changes in wind loads after pruning, especially on large, open-grown, evergreen trees. The objective of this research was to identify the effects of pruning treatments on wind-induced bending moments on Colorado blue spruce (*P. pungens*). Ten, open-grown spruce at the Colorado State Forest Service Nursery (CSFS) in Fort Collins, Colorado were monitored before and after a series of pruning treatments. Trees were pruned to raise or thin crowns over a range of severities between 0% and 40%. Axial trunk deformation was measured using two displacement probes installed orthogonally on each tree, and each displacement probe was calibrated using a static pull test to convert trunk deformations to bending moments. Wind conditions and trunk bending moments were simultaneously monitored and continuously recorded from July 2023 through January 2024. At a given wind speed, mean wind loads did not differ between pruning treatments, but pruning severity significantly affected wind loads. Mean separation analyses were conducted at wind speeds of 10 $m \cdot s^{-1}$, 12.5 $m \cdot s^{-1}$, and 15 $m \cdot s^{-1}$, representing the upper range of 30-minute maximum winds during all severity periods. Compared to the other severities, the average 30-

minute maximum wind-induced bending moments decreased significantly after deadwood removal at the higher wind speeds (12.5 and 15 $m \cdot s^{-1}$). At 10 $m \cdot s^{-1}$, bending moments were significantly lower after deadwood removal compared to the 20% severity period, but no differences were observed among other severity levels. These findings suggest that arborists should carefully consider the amount of material removed from large, open-grown evergreens to reduce wind loads and mitigate tree failure risks. Further research is needed to assess the long-term impact of pruning on tree health and whether the mechanical benefits align with aesthetic expectations in urban greenspaces.

ACKNOWLEDGEMENTS

I would like to express my deepest thanks to all those who have supported me throughout graduate school and especially during the process of completing this thesis.

First and foremost, I extend my heartfelt gratitude to my advisor and fellow tree enthusiast, Dr. Daniel Burcham, for his invaluable guidance, encouragement, and expertise. His insightful feedback, patience, and unwavering support have been instrumental in shaping this work. Thanks for putting your faith in me and encouraging me to strive to be a better arborist and scientist.

I am also grateful to the members of my thesis committee, Dr. Yanlin Guo, Dr. Brian Kane, and Dr. Anthony Koski, for their time, constructive criticism, and suggestions which have greatly enhanced the quality of this research.

A tremendous amount of love and gratitude to my spouse, Samantha Rosado. Words can't begin to describe all you've done to support me through one of the most challenging times in my life. Thank you for always saying "YES" to helping me prune trees in 20° F, drag brush in 95° F, and proofread all my emails and dumpster-fire writing…all while working towards your PhD. I'll cherish all the time we've been able to spend together in grad school, and the lessons I've learned from you about slowing down and living in the present moment. I don't know how you

do it, but thank you, thank you, thank you for keeping me grounded and extending me more grace, love, and understanding than any one person deserves.

Special thanks go to my family members of the Craver Lab: Samantha Rosado, Anthony Percival, Courtney Dunbar, Oliver Fulton, and of course Dr. Joshua Craver. I would not have survived this experience without your constant support, laughter, and endless supply of LOTR and Star Wars quotes. Games nights will forever live in infamy as will “tom-bombadillery” and Josh’s pro-gaming tips.

To my fellow tree-climber, friend, “beast-from-back-East”, and owner of East Side Tree Care LLC., Stuart Rienhoff, thank you. I could not have completed the pull tests without you. All the blood, sweat, and tears (mostly mine from watching you climb up 10 unpruned blue spruce) you shed in the name of research did not go unnoticed…I’ll try to talk Dan and the committee into presenting you with an honorary Master’s. You have my gratitude for keeping me tethered to the industry and tree climbing.

I would like to acknowledge the support of the Colorado State Forest Service Nursery, specifically Scott Godwin and Orion Aon, for providing a site and trees which facilitated my research.

Sarah Wilhelm, thank you for all your assistance in setting up and breaking down the instrumentation out at the research site. I’ll cherish our espresso conversations and thank you

for being open to discussions surrounding issues of DEI in our department and the world at large. I'll work on getting that Burcham Lab t-shirt to you.

To my friends in "Laradise", Jeff Smith and Emily Parsons, owners of TigerTree, Inc., I'm so very grateful for your continued support. Thank you for encouraging me to return to school even when it meant losing an employee. Your generous contributions towards this project ensured the success of this experiment…and that there isn't a huge pile of brush waiting to be chipped out at the Colorado State Forest Service Nursery.

Lastly, I owe a debt of gratitude to my parents, Steve and Sherry Leinbach, for their constant encouragement and patience throughout this endeavor. Their love and support have been an unwavering source of strength.

Thank you all for being an integral part of this journey!

David

DEDICATION

To Jim Savage, who first cultivated my passion for trees and love of tree climbing, and to all the arborists, climbers, urban foresters, and tree nerds who urged me to "go out on a limb". You continually inspire me to climb to new heights.

TABLE OF CONTENTS

LIST OF TABLES

LIST OF FIGURES

CHAPTER 1 – INTRODUCTION

In an era where human activity has been the dominant influence on climate and the environment, the importance and necessity of urban forests is a topic gathering the attention of world leaders and decision makers. With an estimated 70% of the world's population predicted to live in cities by 2050 (Salbitano et al., 2016), the challenges of concentrated populations, such as access to clean water, pollution-related health issues, and public safety, need to be addressed with efficient and effective solutions (Turner-Skoff & Cavender, 2019). Greenspaces, particularly areas where people have access to plant, maintain, and protect trees, have been identified as one solution (United Nations, 2015) to increased urbanization because of the numerous direct and indirect benefits of trees (Elmendorf, 2008; T. Endreny et al., 2017; T. A. Endreny, 2018).

Urban trees offer communities a multitude of benefits. Davies et al. (2017) found that green infrastructure, in particular urban trees, offers the greatest regulation of ecosystem services, including management of stormwater run-off, alleviation of urban heat sinks, and enhanced air quality. For instance, an estimated 711,000 metric tons of air pollution is removed annually from the contiguous United States by urban trees (Nowak et al., 2006). Beyond air pollution removal and oxygenating the atmosphere, trees play a pivotal role in regulating climate patterns (Pramova et al., 2012), improving soil health (Bargali et al., 2019; Chauhan et al., 2018), and supporting biodiversity (Barrios et al., 2018; Threlfall et al., 2017). While these tangible benefits have been examined extensively, recent literature has increasingly emphasized the aesthetic value of trees in urban landscapes and their contributions to enhanced mental health and personal well-being (Sander et al., 2010; Turner-Skoff & Cavender, 2019). Urban

greenspaces have also been found to support physical and psychological health (Salmond et al., 2016), providing people with areas for recreation, physical activity, and socialization. Additionally, Tzoulas et al.'s (2007) literature review found qualitative evidence supporting the reduction of stress, anxiety, aggression, and mental fatigue after spending time in green settings.

Despite these benefits, trees also present several challenges and hazards to urban communities. In the last decade, an increasing number of studies have been published examining what some authors describe as the cost of urban greening or the "ecosystem disservices" of trees (Cariñanos et al., 2017; Conway & Yip, 2016; Delshammar et al., 2015). Cariñanos et al. (2017) identified numerous negative impacts of trees and tree planting including the introduction of non-native or invasive species, pollen-related allergies, maintenance costs (pruning, removal, removal of debris, damage to infrastructure), social hazards (habitat for crime and animals), and, most notably, safety concerns (property damage, personal injury, litigation, and death). According to Schmidlin (2009), wind-related tree failures resulted in 407 deaths in the United States from 1995 to 2007, and Mortimer and Kane (2004) argued that the heightened litigation surrounding tree failures has increased and is expected to continue. Thus arborists, urban foresters, and practitioners aim to strike a balance that safeguards both human safety and the environmental benefits provided by trees in urban spaces.

In the field of arboriculture, tree risk assessment is a common method used to limit the public's exposure to the potential dangers of urban trees. It is a procedure used to systematically evaluate the likelihood and consequences of tree failure (Smiley et al., 2017).

Once a risk assessment has been completed, arborists and urban foresters use the results of the assessment to make informed decisions about how to manage the risk posed by the evaluated tree(s). A hazardous tree with extreme consequences of failure will likely be removed. However, tree removal can often be avoided with effective tree risk management strategies, such as pruning (Lilly et al., 2019; Pavlis et al., 2008) that mitigate potential risks.

Urban trees are commonly pruned for a variety of reasons (Burcham et al., 2020; Pavlis et al., 2008). However, pruning is frequently prescribed as a means of reducing risk associated with wind damage to trees (Gilman et al., 2008a). Despite considerable research on the interaction between trees and wind, few studies have examined the effect of arboricultural pruning treatments on a tree's response to wind (Gilman et al., 2008a). Consequently, the pruning types and standards developed by arborists have largely been adopted without thorough empirical testing (Pavlis et al., 2008). In practice, arborists often determine the severity of pruning visually (American National Standards Institute (ANSI), 2023), and the subjective judgements are often inaccurate (Koeser & Smiley, 2017; Norris, 2007; Stewart et al., 2013). Existing research examining the effects of pruning on wind loads has largely focused on small, deciduous trees grown in nursery settings (Gilman et al., 2008a, 2008b; Pavlis et al., 2008; Smiley & Kane, 2006). Apart from one wind tunnel study (Rudnicki et al., 2004), no research has examined the effect of pruning on wind loads for individual conifers. More work needs to be conducted to understand the effectiveness of pruning as a risk mitigation strategy on open grown trees, especially on evergreens.

While deciduous, broadleaves are more abundant in urban forests and landscapes throughout the United States (Ma et al., 2020), many acknowledge the accumulation of

environmental benefits from coniferous evergreens with year-round physiological activity (Clapp et al., 2014). *Picea pungens* Engelm., commonly known as Colorado blue spruce is widely appreciated and planted in many areas of the United States. The tree was originally discovered by botanists in Colorado, where it was later recognized as the state tree in 1939. Unfortunately, many practitioners have noticed the susceptibility of mature Colorado blue spruce to windthrow, and there is a need to effectively mitigate risks associated with such trees during strong winter storms. Thus, the objectives of this study were:

1) to evaluate the effects of pruning type and severity on the wind-induced bending moments of Colorado blue spruce and
2) to use the results of the experiment to recommend strategies for pruning Colorado blue spruce trees to mitigate the risk of wind-induced failures.

CHAPTER 2 – LITERATURE REVIEW

Tree-Wind Interaction

From germination until death, wind is the largest force acting on a tree (K. R. James & Kane, 2008). The dynamic nature of wind causes trees to adapt to varying magnitudes of mechanical loads (B. Gardiner & Quine, 2000; Mattheck & Breloer, 1994), leading to adjustments in their structural integrity, growth patterns, and overall survival (Archer, 2013; Ennos, 1997). Trees, like all organisms, obey the laws of physics. As a tree grows, the resulting increase in crown frontal area translates to increased drag (F_d), shown by the equation:

$$F_d = \frac{1}{2}\rho C_d A U^2, \quad \text{(Eq. 1)}$$

where *p* is air density, C_d is the drag coefficient, A is the frontal area of the tree crown, and U is wind speed. Bending moments (M_B), the product of F_d and center of pressure height (h_{cp}), also increase with tree size as drag acts at progressively greater heights:

$$M_B = F_d h_{cp}. \quad \text{(Eq. 2)}$$

Large bending moments can often lead to structural tree failure, where wind loads exceed the material strength of tree wood. Wood strength varies between tree species (Zobel & van Buijtenen, 1989), and the likelihood of tree failure is greater with the presence of tree defects such as decay (Huang et al., 2017), which reduce a tree's strength or load-bearing capacity.

Research examining tree biomechanics has revealed much about the mechanical responses of trees to drag. Older studies (Fraser, 1962) utilized static methods to explore these responses,

while improving technologies have allowed recent studies to employ dynamic methods of data collection and analysis that more closely investigate actual tree-wind interactions. In existing studies, the mechanical behavior of numerous trees has been studied using a static pull test. It involves attaching a rope to the tree trunk at approximately half the tree's height to apply a static load meant to simulate drag (Brudi, 2002; Clair et al., 2003; Moore, 2000; Neild & Wood, 1999; Peltola et al., 2000; Silins et al., 2000). The known force (kN) exerted by the pull rope attached at a given height (m) on the trunk generates a bending moment (kN·m) at the base of the tree. This result can then be used to estimate the wind velocity needed to uproot a tree or cause structural damage to the trunk. However, according to Hassinen et al. (1998) and Oliver and Mayhead (1974), tree failure has been recorded at lesser wind speeds than predicted by static pull tests, presumably a result of the dynamic forces of wind as opposed to statically applied forces of a pull test.

Drag is both spatially and temporally dynamic and variable. Thus, trees have evolved with drag to be flexible structures, equipped with dynamically swaying trunks and branches to disperse wind loads. Cellulose and lignin, the primary components found in the plant cell wall, are responsible for giving trees rigidity and flexibility, enabling them to grow to great heights without collapsing under their own weight and the force of the wind. Researchers have developed several methods and adapted instruments to measure and record the dynamic interaction between trees and wind, including accelerometers (Blackburn et al., 1988; Burcham et al., 2020; Peltola, 1996), displacement transducers (Burcham et al., 2020, 2021; B. A. Gardiner, 1995; Kerzenmacher & Gardiner, 1998; Milne, 1991; Roodbaraky et al., 1994), lasers (Baker, 1997), prism-based systems (Hassinen et al., 1998), strain gauges (Angelou et al., 2019;

Guitard & Castera, 1995; K. R. James & Kane, 2008; Moore & Maguire, 2005; Murphy et al., 2005; Watson, 2000), tilt sensors (Flesch & Wilson, 1999; Rudnicki et al., 2001), and video-based technology (Peltola, 1996).

Some studies conducted in the last five years have utilized linear variable displacement transducers (LVDTs), more commonly referred to as displacement probes, to record the dynamic motion of trees in the wind (Burcham et al., 2020, 2021). These instruments accurately and precisely measure bending induced strain of the lower tree trunk caused by the wind. The LVDTs used in Burcham et al.'s (2020, 2021) experiments reported a strain resolution of 43 $\mu m\ m^{-1}$ with probes measuring 20 mm displacement over a linear distance of 226.9 mm. Strains on the trunk measured during wind events were converted into bending moments after measuring strains during a static pull test to calibrate strain with applied bending moment. Older studies (Brudi, 2002; Peltola et al., 2000) have utilized displacement transducers of similar design in static pull tests, but were not described in great detail. These instruments have enabled researchers to scientifically describe and visually represent the dynamic relationship between trees and the wind, and in doing so has aided researchers in looking at the mechanical effects of tree pruning as it relates to wind-induced deformations.

Tree Pruning

Trees are pruned for a variety of reasons, such as providing clearance to structures, rights-of-way and above-ground utilities, enhancing natural views (vista pruning), improving overall aesthetics, and encouraging proper branching architecture (Lilly et al., 2019). Trees are often pruned to mitigate the risk of wind damage (Burcham et al., 2020, 2021; James & Kane,

2008; Smiley & Kane, 2006). As such, in the United States, trees were historically topped and lions-tailed – two pruning practices thought to reduce the risk of tree failure by decreasing drag and facilitating wind passage through the tree crown with increased porosity, respectively (Pavlis et al., 2008). Tree topping (**Figure 1**) is a process by which tree height is reduced with the expectation of limiting leverage exerted on a tree trunk by the wind, and lions-tailing (**Figure 2**) is technique that involves the removal of a tree's interior foliage, resulting in bare branches and limbs that extend out to tufts of terminal growth. These pruning types are no longer recommended (American National Standards Institute (ANSI), 2023). Karlovich et al. (2000) found that the indiscriminate removal of the upper tree canopy, with no regard for placement of reduction or heading cuts, resulted in poor wound closure, increased vulnerability to diseases

Figure 1. Examples of topped trees (Advanced Tree Care, Inc., 2024).

and pests, decay, and prolific sprouting. Lions-tailing often over elevates the crown, positioning the crown mass near the top of the canopy. This increases the leverage on the branch tips, where drag exerts force, resulting in a larger bending moment (Gilman et al., 2008b). Rottmann's (1985) experiment showed that this type of pruning leaves most of the tree canopy farther from the ground, increasing the tree's center of gravity and the likelihood of failure from increased forces experienced at branch unions and at the base of the tree (Peltola et al., 1999). Additionally, Smiley and Kane (2006) found evidence that suggests that per unit of crown mass removed, reduction pruning, the intentional shortening of tree canopy height and/or width, more effectively reduced the likelihood of tree failure than lion's-tailing. Reduction pruning aims to avoid the negative effects of topping by intentionally placing heading cuts near a lateral limb,

Figure 2. Example of lions-tailing (Conlon, 2024)

approximately one-third the diameter of the cut stem (American National Standards Institute (ANSI), 2023; Lilly, 2001; Lilly et al., 2019).

Today, arborists in the United States adhere to the International Society of Arboriculture's (ISA) Best Management Practices-Pruning (Lilly et al., 2019) and the A300 Standard (American National Standards Institute (ANSI), 2023), which require the use of different pruning techniques to achieve specific objectives, such as the mitigation of wind damage. Reducing the likelihood of tree failure from the wind is often accomplished by selectively removing branches or leaf area to improve crown structure and porosity or decrease drag (Lilly et al., 2019). The relationship between mass and drag in existing studies implies that drag can be minimized with increasingly severe pruning (Pavlis et al., 2008; Smiley & Kane, 2006). However, excessive pruning performed to decrease drag also led to adverse physiological tree effects such as wood decay, altered growth patterns, weak branch attachments, and modified carbohydrate allocation (Hamzah et al., 2021; Suchocka et al., 2021). Thus, arborists and urban foresters aim to strike a balance between risk mitigation and tree health and appearance.

To avoid the adverse effects of excessive pruning, the ANSI A300 (Part 1) was written to mandate a limit to the amount of live material that practitioners should remove from a tree in one annual growing season. In previous iterations, the standard stated that no more than 25% of live material should be removed from a tree each year. As of 2023, the standard was rewritten to include more flexible language and lacks a specific figure, likely to account for the difficultly in standardizing a visually-subjective process or to avoid the difficulty of specifying a universal limit for diverse pruning objectives. Without a realistic method to standardize the

material removed from a tree, arborists consistently met and often exceeded the recommendation laid out in the A300 standard (Koeser & Smiley, 2017; Norris, 2007; Stewart et al., 2013). More research is needed to develop consistent and accurate pruning metrics for field use.

Mechanical Consequences of Tree Pruning

In arboriculture, two commonly used pruning techniques—crown reduction and thinning—aim to reduce the likelihood of failure. Smiley and Kane (2006) conducted a study on the effects of these pruning methods on young red maple trees (*Acer rubrum*). They examined four treatments: thinning, reduction, lions-tailing (excessive raising), and leaf stripping. Drag was generated by strapping the pruned trees to a frame on a moving truck, while wind and force data were recorded. Results indicated that all pruned trees experienced lower wind loads than unpruned ones, and significant differences were found among the pruning types. Limitations of the study included small wind loads, artificial conditions, and a focus on immature trees. Nevertheless, this research provided valuable baseline data for future studies in the field.

Pavlis et al.'s (2008) experiment examined the effects of three pruning types—raising, thinning, and reduction—at 25% severity, across three different deciduous tree species - Freeman maple (*Acer × freemanii*), swamp white oak (*Quercus bicolor* Willd.), and shingle oak (*Quercus imbricaria* Michx.). Methodology was similar to Smiley and Kane's (2006) experiment and also included mass measurements to illustrate the effect of different pruning types, since mass is predictor of drag and bending moment (Rudnicki et al., 2004; Smiley & Kane, 2006;

Vollsinger et al., 2005). This study found that pruning treatments significantly reduced wind loads compared to unpruned trees, largely because of the reduction in tree mass. Limitations of this study included the use of immature trees, difficulty replicating wind conditions strong enough to cause tree damage or failure, and trees were separated from their root systems. Young tree canopies tend to differ in their ability to manage drag from their mature counterparts, with increased stem flexibility and crown deflection and reconfiguration (Smiley & Kane, 2006). Bending moments observed in this experiment, where experimental trees were cut above the root flare and attached to a metal sled to mimic tree roots, may not accurately reflect the bending moments of trees still connected to their roots. While this methodology attempts to replicate some aspects of a tree root system, it may not fully capture the complexity and interactions of actual roots, which play a significant role in overall stability, trunk stiffness, and structural integrity.

Gilman et al.'s (2008a) study achieved greater maximum wind speeds (> 45 $\mathrm{m{\cdot}s^{-1}}$) by means of airboat propeller. The mobile propeller allowed 20 live oak (*Quercus virginiana* 'Cathedral Oak') trees to remain in the ground during the experiment. Three strain gauges were positioned in each subject tree – top, middle, and bottom of canopy. Dividing each tree canopy allowed for more uniform removal of pruned material, which was confirmed by total foliar weight. Pruning types examined in this study were crown raising, reduction, and thinning with a pruning severity of 33%. Thinning and reduction pruning types were found to be the most statistically effective in reducing trunk movement. Limitations of this study were similar to previous studies (Pavlis et al., 2008; Smiley & Kane, 2006), but also included trees that were

taller than the wind field created by the propeller. Additionally, these studies did not examine the long-term effects of pruning on wind loads.

Burcham et al. (2020, 2021) investigated the impact of pruning on mature tropical trees, specifically focusing on Senegal mahogany (*Khaya sengalensis*) and rain tree (*Samanea saman*). The 2021 study explored two pruning types—raised and reduced—across three severities (0%, 10%, and 20%). A detailed pruning methodology was developed to ensure consistency and accuracy in achieving desired severities. Data on displacement and wind were collected to evaluate bending moments and tree health. The results indicated that reduced trees experienced less wind loading and, consequently, a lower risk of failure compared to thinned trees. Low wind speeds limited the study, confining observations to mild, non-destructive conditions. Overall, while reduced pruning enhances stability and decreases failure risk, it may negatively affect crown health, necessitating a careful balance for tree longevity.

While growing knowledge continues to develop around pruning's use in mitigating wind damage and the consequences of that damage for deciduous trees, few studies have examined the effects of pruning on evergreen trees. Even fewer experiments have examined the effects of pruning on mature, open-grown evergreens. Therefore, the proposed study will investigate the following hypothesis on large, open-grown Colorado blue spruce (*Picea pungens*):

1) Raising trees will be a less effective method for reducing bending moments compared to thinning trees and
2) bending moments will decrease with increasing severity of both pruning treatments.

CHAPTER 3 – METHODOLOGY

Research Site and Trees

Ten mature Colorado blue spruce (*Picea pungens*) were selected for this study from a windrow of 40 trees – 18 *P. pungens* and 22 ponderosa pine (*Pinus ponderosa*) – located at the Colorado State Forest Service (CSFS) Nursery in Fort Collins, Colorado (**Figure 3**). The age of the trees was unknown because planting records did not exist. Even though the exact age of the spruce trees is unknown, they can be considered "mature" based on observable traits such as their large size, stable structure, reproductive capacity, and slowed growth rate, all of which indicate they have reached full development. The windrow was not maintained by the CSFS,

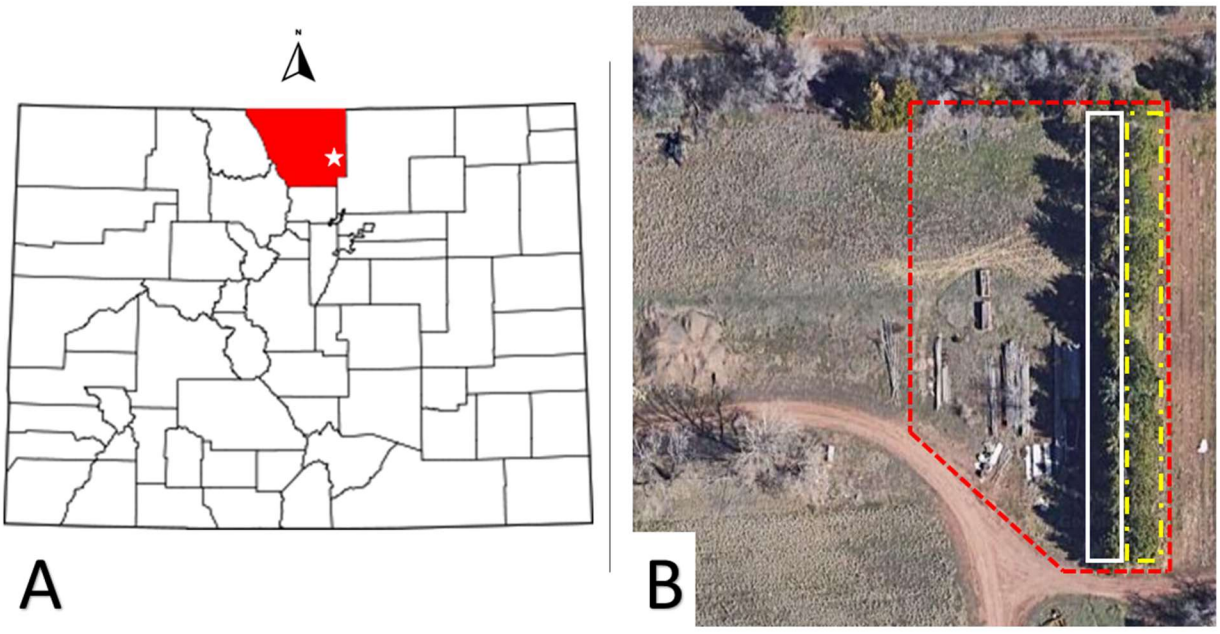

Figure 3. **A** Research site (star marker) located at the Colorado State Forest Service Nursery (40°35'15.9"N, 105°08'27.6"W, elevation 1,564 m, USDA Hardiness Zone 5b). **B** Borders of the site (outlined in red, dashed line) with subject trees located in N-S windrow (outlined in solid, white line) and neighboring pine row (outlined in dash-dot, yellow line).

and, in the absence of pruning, tree form and growth habit were typical of open grown spruce with an excurrent, conical-shaped canopy extending from the ground to the top of the tree.

The 22 pines were located 3.7 m east and parallel to the North-South row of spruce (**Figure 3**). The rows of spruce and pine existed on opposing sides of an inactive irrigation ditch (**Figure 4**) that was not utilized during the experiment (July 2023 to January 2024). The spruce and pines were pruned to minimize branch and canopy collisions between adjacent trees during wind-induced tree movement.

Open-grown spruce trees with healthy crowns and even branch spacing were selected for the experiment. Several morphological characteristics (**Table 1**) of each spruce were recorded, including tree height, crown length, and diameter at breast height (DBH) or 1.37 m above grade.

Table 1 Morphological data of spruce (*P. pungens*) grouped by pruning treatment. Mean values (SD) are shown.

Pruning Treatment	N	Tree Height (m)	Crown Length (m)	DBH (cm)
Raised	5	12.66 (1.29)	12.62 (1.36)	44.14 (4.59)
Thinned	5	13.42 (1.19)	12.93 (1.46)	40.91 (3.55)

The climate of the research site is typical of Colorado's Front Range (Hansen et al., 1978), which is a semi-arid region characterized by warm, dry summers and cold, snowy, windy winters *(Colorado Climate Center - Colorado's Climate, n.d.*). Throughout the year, temperatures vary from -7° C to 35° C, and daily temperature ranges can span up to 30° C.

Average annual rainfall for this area is 43.66 cm (*NOAA NCEI U.S. Climate Normals Quick Access*, n.d.). A prevailing westerly wind is common throughout the year with wind speeds varying seasonally. The windiest time of the year is typically November through April, with average wind speeds of 5 $\mathrm{m{\cdot}s^{-1}}$ (*Colorado Climate Center - Colorado's Climate*, n.d.).

Instrumentation

A three-dimensional ultrasonic anemometer (Model 81000, R.M. Young Company, Traverse City, MI, USA) was used to measure wind velocity. The anemometer was installed on a 14.6 m weather mast (PA2 – Transportable Mast System 3-Way Halyard, South Midlands Communications Ltd., Eastleigh, Hampshire, England) at the average height of experimental trees (13.1 m). The weather mast was erected 15 m west from the middle of the row of experimental trees (**Figure 4**). The anemometer measured wind speed within a range of 0 to 40 $\mathrm{m{\cdot}s^{-1}}$ with a resolution of 0.01 $\mathrm{m{\cdot}s^{-1}}$ and accuracy equivalent to $\pm\ 3\ \%$ of output; and it recorded wind direction within a range of 0.0 to 359.9° with a resolution of 0.1° and $\pm$ 2° (1 to 30 $\mathrm{m{\cdot}s^{-1}}$) or $\pm$ 5° (30 to 40 $\mathrm{m{\cdot}s^{-1}}$) accuracy. A lightning protection system was installed on the mast to mitigate the risk of equipment damage during severe weather.

Axial trunk displacement, x (mm), was monitored by two linear variable displacement transducers (LVDT) (VS/20/U, Solartron Metrology, West Sussex, UK) mounted orthogonally on the tree trunks at 1.37 m above grade (**Figure 5**). Secured to the trees using hanger bolts, the probes measured both elongation and contraction of the outer wood during wind-induced bending. One LVDT was mounted on the east side of the tree and the other on the north side.

The probes measured 20 mm total displacement over a linear distance of 225.5 mm with a measurement resolution of 10 μm and accuracy equivalent to 0.20% of output. Strain resolution of each LVDT was approximately doubled from 44 $\mu m \cdot m^{-1}$ to 23 $\mu m \cdot m^{-1}$ by adding a 200 mm segment of threaded rod to the LVDT body (**Figure 5**).

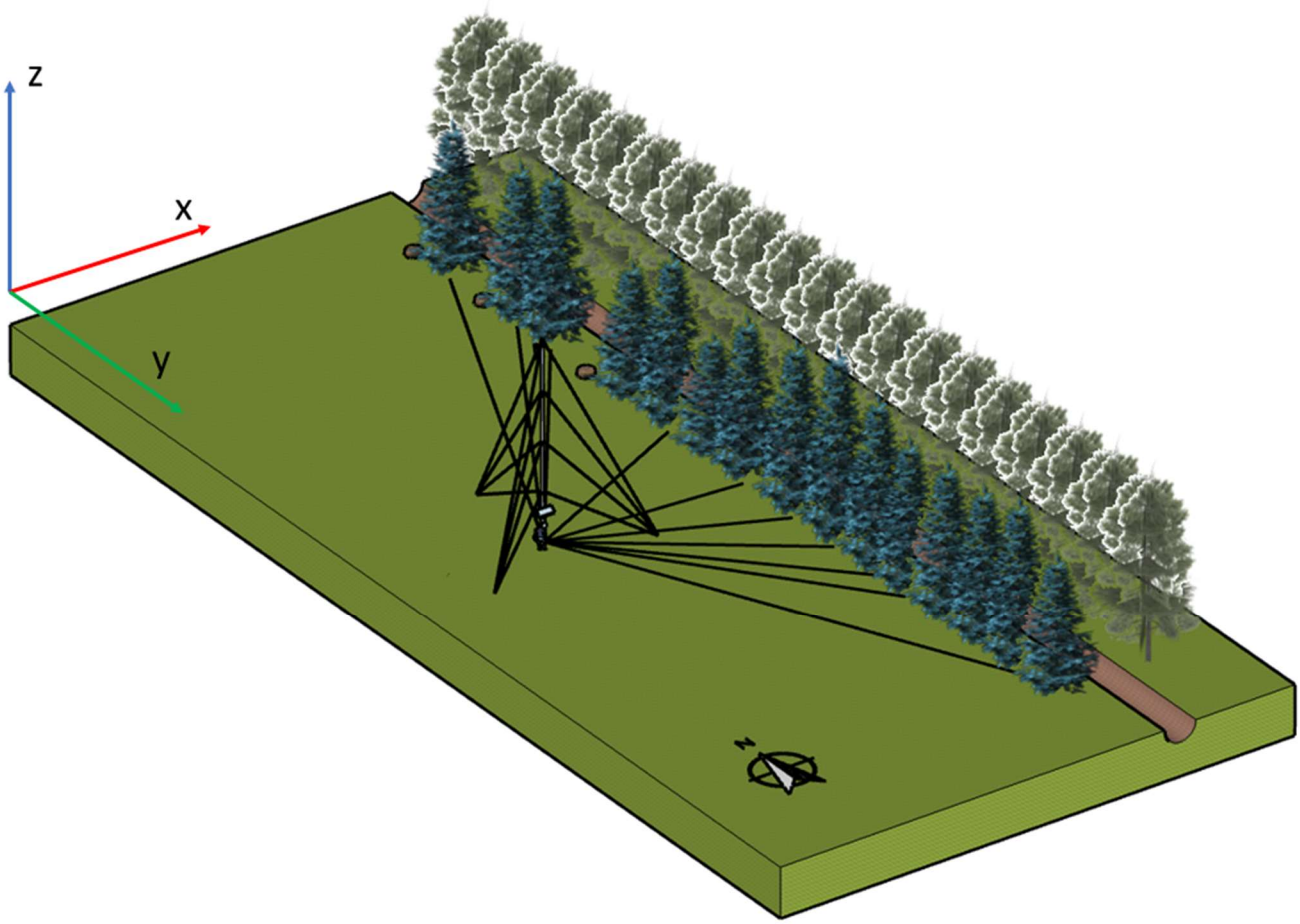

Figure 4. Site and instrumentation layout. Figure not to scale.

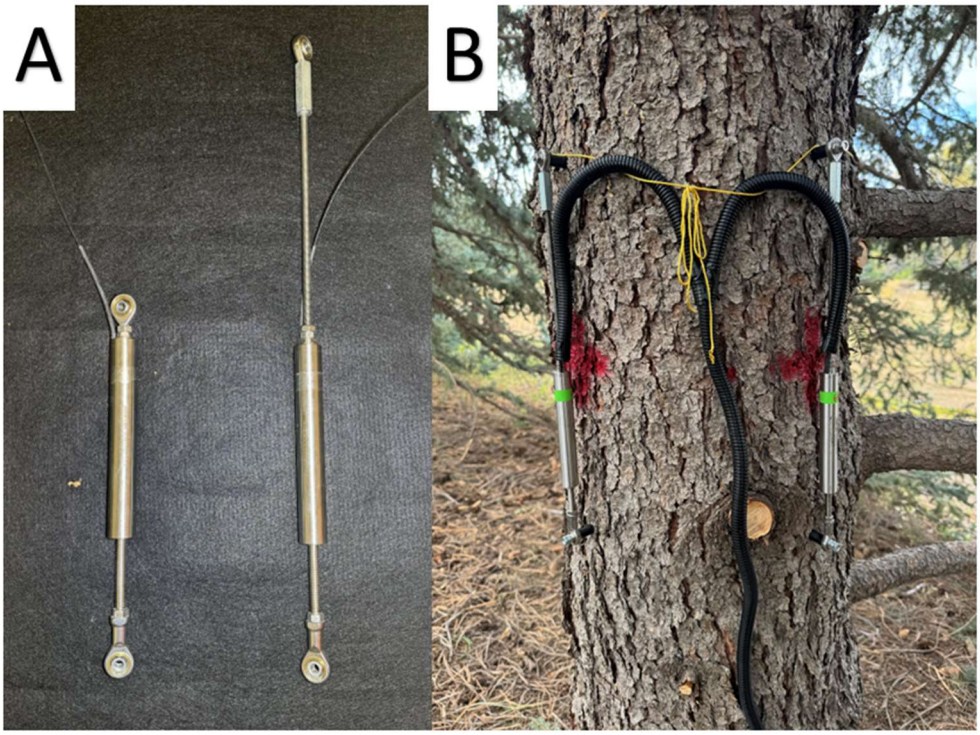

Figure 5. A Original (left) and modified LVDT (right). **B** Pair of LVDTs mounted at approximately mid-stroke on North (0°) and East (90°) of subject tree, showing typical setup of all test trees. Flexible conduit was installed around probe wiring to prevent mammal damage. Wiring and conduit secured over top hanger bolts to prevent gravitational tension.

Data Collection and Power Supply

Wind velocity, $\boldsymbol{u}$ ($\mathrm{m \cdot s^{-1}}$), and x were simultaneously and continuously recorded at 20 Hz from July 2023 to January 2024 at the experimental site. The 20 LVDT probes and anemometer were wired to analogue and digital channels, respectively, on two dataloggers (CR1000 and CR1000X, Campbell Scientific Inc., Logan, UT, USA) mounted on the weather mast inside a weather resistant enclosure (ENC10/12, Campbell Scientific Inc., Logan, UT, USA). The entire system was powered by a sealed lead acid battery (40701, Grainger, Kansas City, MO, USA), which was housed in a commercial grade battery box (HM-484 by The NOCO Company,

Glenwillow, OH, USA) and insulated to protect against temperature fluctuations. Battery charge was maintained through a 90-watt solar panel (SP90-L15-P, Campbell Scientific Inc., Logan, UT, USA) mounted 0.5 m above the weather resistant enclosure on the mast, and power management was controlled through a charge regulator (CH200, Campbell Scientific Inc., Logan, UT, USA) (**Figure 6**).

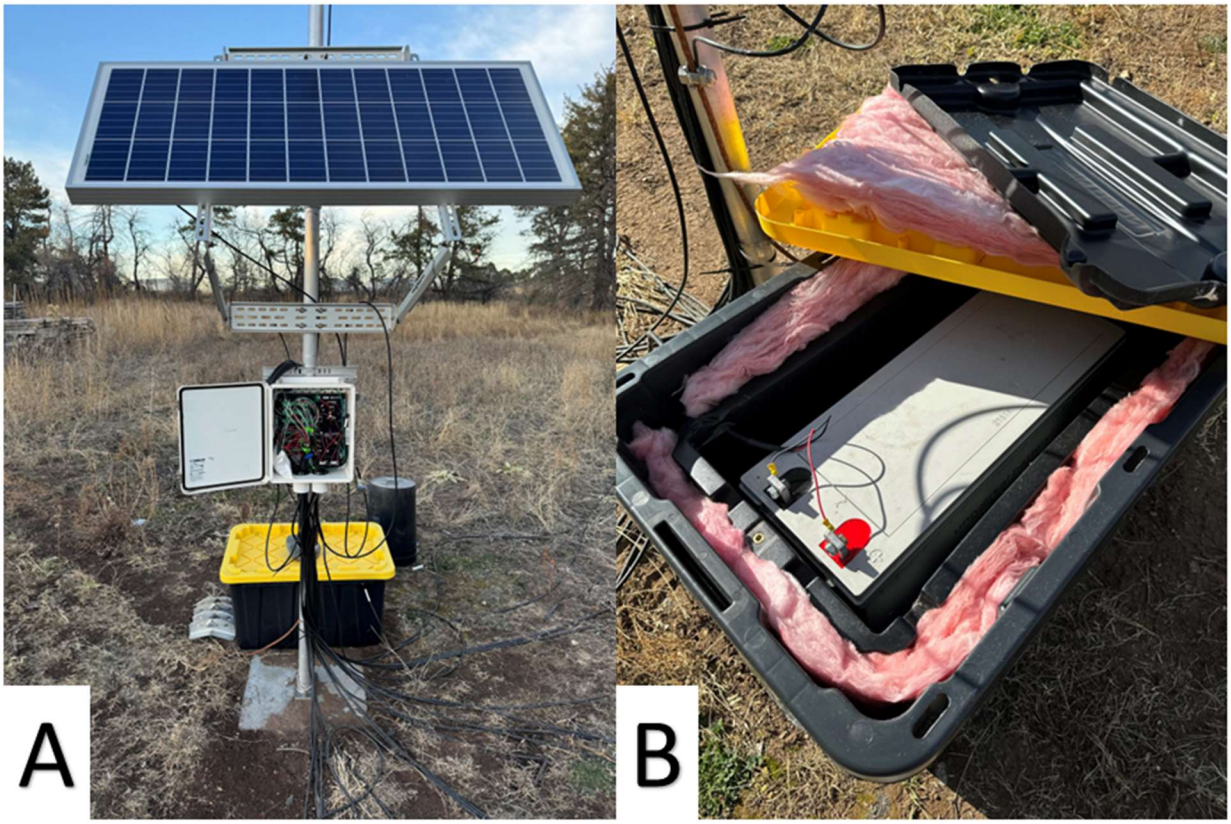

Figure 6. Power and data collection system (A) with insulated battery (B) to regulate against temperature fluctuations at site.

LVDT Calibration - Pull Tests

To characterize the relationship between x and wind-induced bending moments, M_B (kN·m), a calibration coefficient, C_1 (kN·m/mm), was determined for each pair of LVDTs assigned to each experimental tree using a series of static pull tests (Wellpott, 2008). Force and

displacement data were recorded continuously at 20 Hz during pull testing (**Figure 7**); a load shackle measured load forces exerted on the tree while the eastern displacement probe recorded the displacement, x_{E-W} (mm), of the lower tree trunk. A pulling force (kN) was applied from the West to each tree with a rope attached to the trunk at half-tree height. This ensured the pull-induced trunk displacement were aligned incident to the LVDT secured to the eastern side (tension side) of each tree. Loads were generated by a 2-to-1 mechanical advantage system where the pull rope (9/16" Stable Braid Bull Rope, Samson Rope Technologies, Ferndale, WA, USA) was doubled through a pulley (10 Ton Snatch Block, TICONN, China) secured to a load shackle (ISHKB3.25MT1361, Interface Force Measurement Solutions, Scottsdale, AZ, USA), and attached to the tree by an arborist dead-eye sling (5/8" Stable Braid Bull Rope, Samson Rope Technologies, Ferndale, WA, USA). A winch (VR Evo 8-S, Warn Industries, Inc., Clackamas, OR, USA) attached to a pickup truck was used to generate the force (kN) needed to displace the upper tree canopy and induce a bending moment on the lower tree trunk. The pull rope was terminated under the winch, parallel to the direction of pull. The incremental M_B generated at the middle of the displacement probe was calculated as:

$$M_B = F\cos\theta l \quad \text{(Eq. 3)}$$

where F is the force (kN) applied by pull rope; θ is the degree angles between the pull rope attachment point and a horizontal plane drawn from the winch to middle of each eastern LVDT (**Figure 8**); and l is the vertical distance (m) between the pull rope attachment point and the mid-point of the displacement probe. C_1 was then calculated as the slope of an ordinary least-squares regression line fit to model M_B as a function of x_{E-W} (Burcham et al., 2021):

$$C_1 = M_B / x_{E-W} \quad \text{(Eq. 4}$$

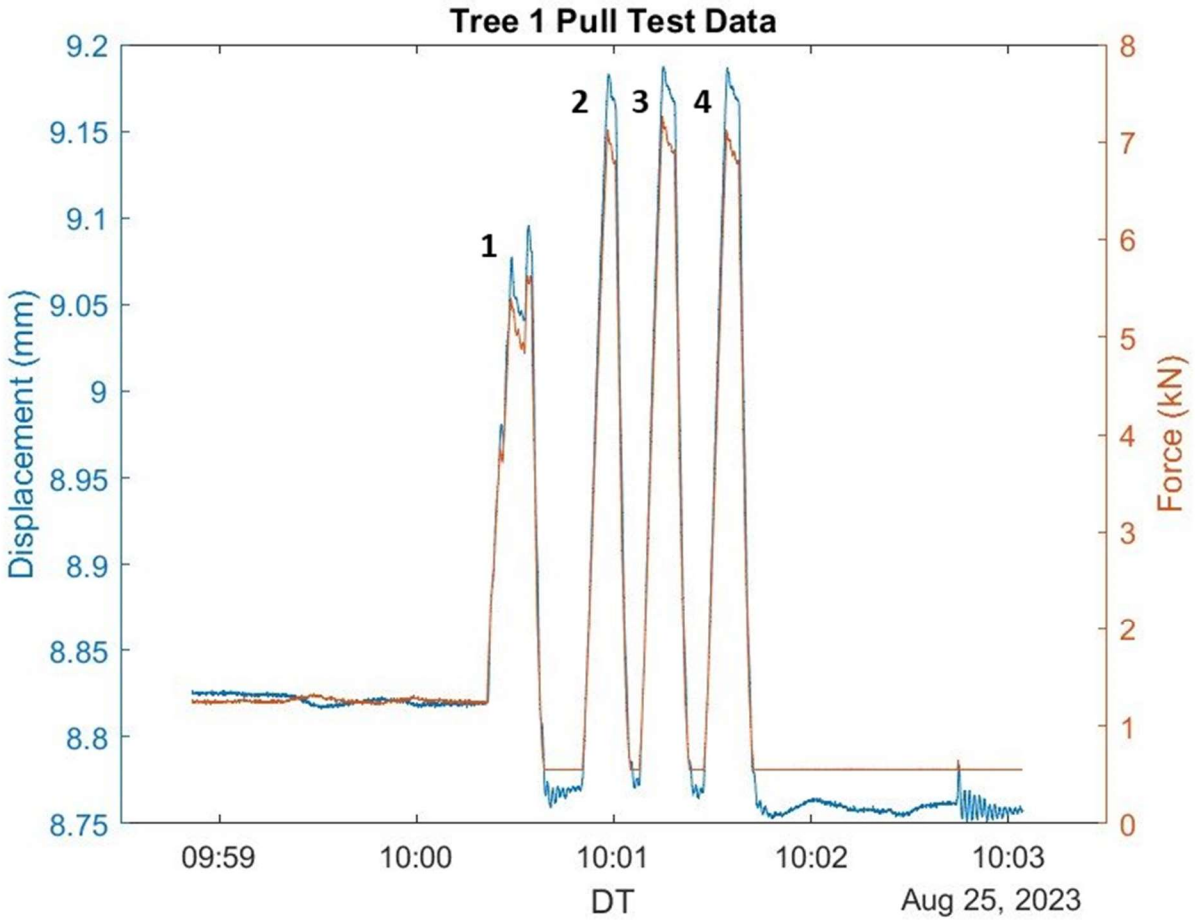

Figure 7 Continuous displacement (left y-axis, blue line) and force (right y-axis, red line) measurements for pull test on August 25, 2023, between 9:59 AM and 10:03 AM at 20 Hz sampling rate. Spiked signals (1-4) represent series of pull tests with each positive slope (left side of each spike).

During some pull tests, the applied load fluctuated abruptly from slack in the rigging system. The tests affected by load fluctuations were detected using residual inspection for a linear model fit to the data and, as necessary, excluded from further analysis.

To estimate trunk stiffness, Young's modulus, E (N m^{-2} = Pa), was calculated as:

$$E = \sigma/\varepsilon \quad \text{(Eq. 5)}$$

where σ (N m^{-2} = Pa) is stress, calculated as the sum of induced bending and axial stress (Kane, 2014):

$$\sigma = {F\sin\theta}/{\pi ab} + {F\cos\theta Lb}/{I}, \quad \text{(Eq. 6)}$$

where F (kN) is an applied force of the pull rope; θ (degrees) is the angle between the pull rope attachment point and a horizontal plane drawn from the winch to the middle of each eastern LVDT, which is parallel to the ground; a and b are the trunk radii perpendicular and parallel to the direction of bending, respectively; L is the vertical distance (m) between the pull rope attachment point and the mid-point of the displacement probe; and I is the moment of area (m^4) determined using:

$$I = {\pi}/{4}\, ab^3. \quad \text{(Eq. 7)}$$

Strain was calculated as:

$$\varepsilon = \Delta l/l, \quad \text{(Eq. 8)}$$

where l is the undeformed length of the LVDT and Δl is the change in the length of the displacement probe during the pull test.

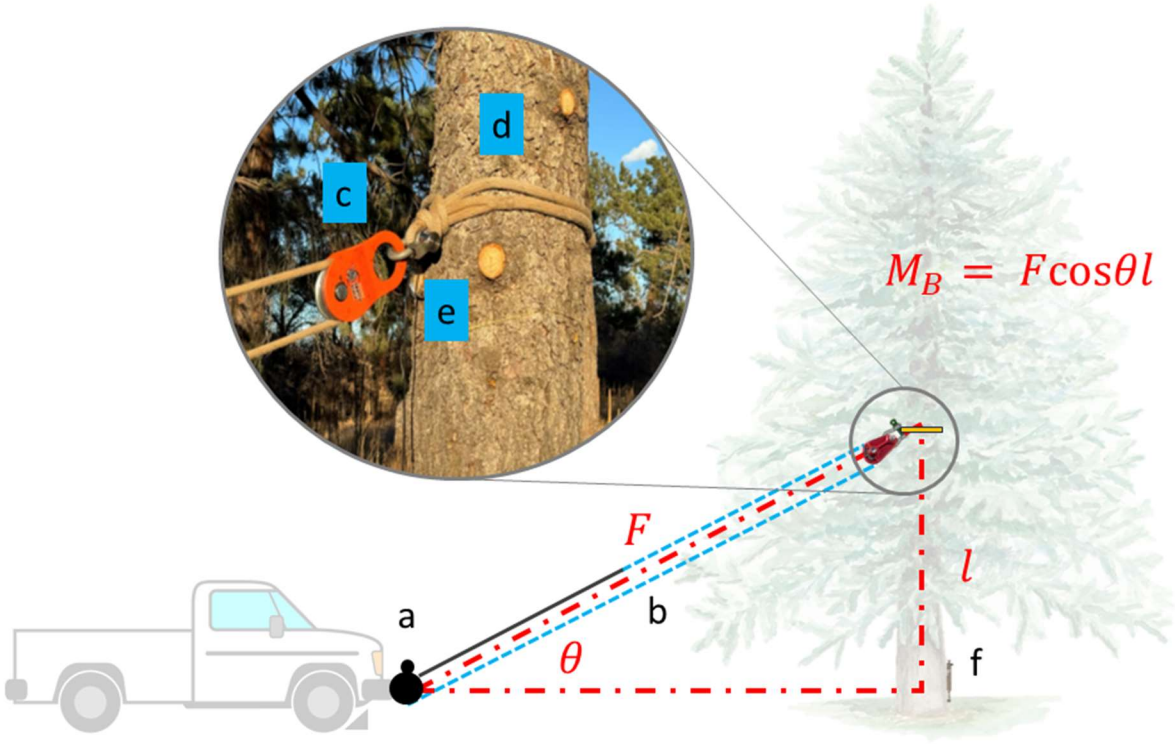

Figure 8. Typical pull test configuration with force (F) generated from the winch (a; solid black line) connected to a pull rope (b; dashed blue line) doubled through a 10-ton pulley (c) and anchored directly beneath the winch to achieve a 2-to-1 mechanical advantage. The pulley was attached at mid-tree height via an arborist sling (d) with a load shackle (e) positioned directly behind the pulley. Trunk displacements were aligned incident by the east facing LVDT (f). Continuous F and displacement data were measured at 20 Hz to calculate continuous bending moments using the formula $M_B = F\cos\theta l$. Figure not to scale.

Pruning Treatments and Severities

Two pruning treatments were examined in this study – crown raising and thinning. These are common pruning methods used by practitioners to achieve specific goals in the urban forest such as clearance for structures and increasing crown porosity, respectively. All pruning performed on trees as part of the experiment was conducted by the same individual for consistency and followed the American National Standard Institute's regulations for Tree Care Operations ANSI A300 (Part 1) (TCIA, 2017). The ten experimental trees were randomly assigned to one of two pruning treatments and progressively raised or thinned to the following severities—0%, deadwood removal, 10%, 20%, and 40%—with each severity maintained for 30 days before progressing to the next severity. All pruning treatments only removed primary limbs. The removal of dead branches was not quantified in this experiment, but all experimental trees contained a similar, substantial amount of deadwood.

Raised trees were pruned from the ground up along the trunk increasing the vertical space between the bottom of the tree crown and the ground. Pruning severity was calculated using the percent change in tree crown height, H_{CROWN} (m). The following formula was used to determine and establish the 10%, 20%, and 40% severities:

$$RAISED_S = H_{CROWN}S, \quad \text{(Eq. 9)}$$

where H_{CROWN} is the vertical distance between the crown apex and lowest branch; and S is the target severity (%) (**Figure 9**). $RAISED_S$ was applied cumulatively at each severity. After the 10% severity, for example, the 20% severity was applied by raising H_{CROWN} an additional 10%.

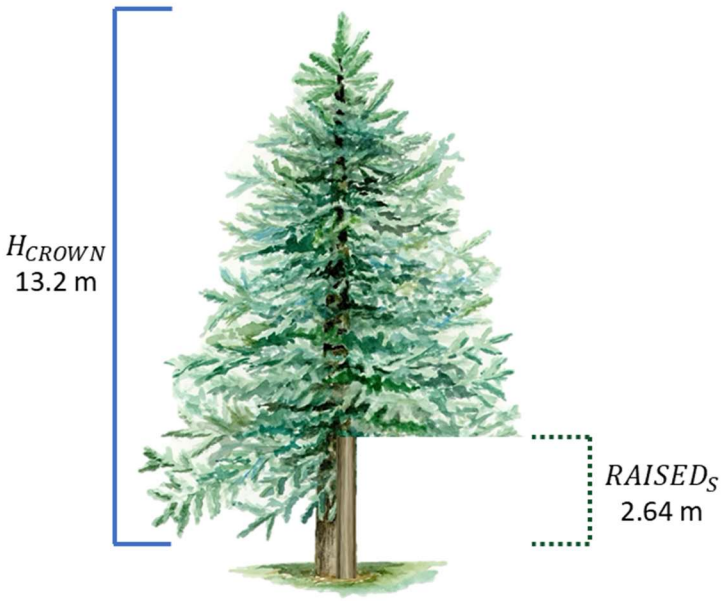

Figure 9 Calculation of 20% raised severity on Tree 1. H_{CROWN} has been multiplied by S (20%) to achieve $RAISED_S$ (Eq. 9). Tree 1 was previously raised to a 10% severity ($RAISED_S$ = 1.32 m). An additional 10% (1.32m) of H_{CROWN} was removed to achieve a cumulative 20% severity.

For thinned trees, the severity of pruning was determined using a crown metric unique to each tree: the cumulative sum of branch diameters, Σ_{DIA} (mm), broadly according to Kane et al. (2014). All primary branch diameters were recorded for each experimental tree using a dial caliper (D15TX, Mitutoyo Corporation, Takatsu-ku, Kawasaki-shi, Kanagawa, Japan), with a measuring range of 0-150 mm and a graduation of 0.02 mm. Starting from the lowest branch, measurements were taken until trunk diameter decreased below 9.5 cm. For consistency, branch diameter measurements were taken at the branch collar with the caliper oriented along

a vertical plane. Σ_{DIA} was then multiplied by each severity S (%) to determine the cumulative branch diameter to be removed from each tree canopy as:

$$THINNED_S = \Sigma_{DIA} S \quad \text{(Eq. 10)}$$

The target severity, S, was subsequently divided into three —parts applied separately to the top, middle, and bottom thirds of the tree crown, H_{CROWN}. Visually, the crown density appeared highest near the top of all trees. To create a more uniform crown density profile during thinning, half of the target severity was applied to the top third of the crown, and the remaining half was split between the bottom two thirds (**Figure 10**).

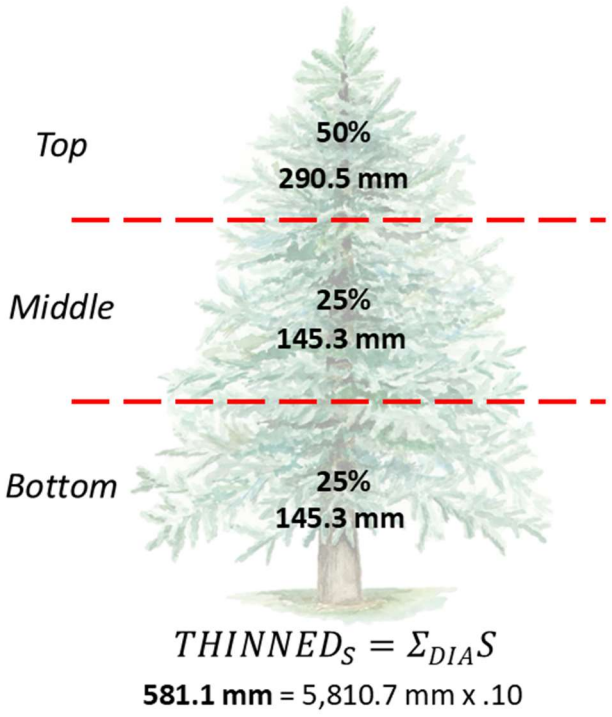

Figure 10 Calculation of 10% thinned severity on Tree 2.

Data Processing and Statistical Analysis

30-minute data intervals were consistently used for analysis to capture significant variation in wind velocity while avoiding noise and fluctuations that might occur in shorter time intervals, as well as slowly varying trends in longer time intervals. Time histories were despiked by identifying trunk displacements more than three local scaled Median Absolute Deviations (MAD) from the local median displacement value over a sliding window of 250 neighboring displacements and replacing identified outliers with the nearest nonoutlier values. Due to freezing temperatures potentially affecting C_1 of each tree, all 30-minute time histories coinciding with temperatures below 0° C were excluded from analysis. Range tests were performed to ensure that recorded displacements did not erroneously exceed the physical 20 mm stroke length of each probe. Intervals where probe range exceeded 20 mm were removed from the study.

Spectral analysis was used to detect and remove displacement signals contaminated by noise. To compute power spectral density (PSD), the mean was removed from 30-minute time histories of displacement, and an ensemble average PSD was computed from eight separate non-overlapping windows with 4,096 observations multiplied by a Hamming window to minimize spectral leakage. After computing PSDs for a given displacement time history, the presence or absence of a prominent peak in PSD between 0.1 and 1 Hz, the frequency range for any tree's fundamental mode of vibration (de Langre, 2019), was used to check signal quality. For 30-minute intervals with average wind speed above 0.5 $\mathrm{m{\cdot}s^{-1}}$, the absence of a prominent peak in the decihertz range was assumed to be caused by noise, and the time history was excluded from further analysis. Finally, displacement time histories were numerically

differentiated to confirm that actual measurement resolution did not exceed the sensor's specifications (i.e., 0.001 mm).

Using the assumption that drag primarily acts along the prevailing wind direction (Mayer, 1987; Schindler, 2008), 30-minute intervals of $\boldsymbol{u}$ (i.e., $[u_x, u_y, u_z]$) were rotated about u_z to align with the prevailing wind direction (30-minute modal direction of $\boldsymbol{u}$). The rotation of $\boldsymbol{u}$ about u_z produced u, v, and w scalars of streamwise, cross-streamwise, and vertical wind velocity components, respectively. To analyze streamwise trunk displacement, 30-minute intervals of $\boldsymbol{x}$ were similarly rotated to align x_{E-W} with the prevailing wind direction. After mean removal, trunk displacement was multiplied by C_1 to obtain M_B.

To select the wind statistic most closely related to the measured tree response for use in statistical analysis, the relationship between trunk displacement and several wind statistics, computed over the same 30-minute intervals, were investigated. In total, six wind statistics were evaluated: mean u, maximum u, mean $|\boldsymbol{u}|$, maximum $|\boldsymbol{u}|$, and mean and maximum momentum flux, M ($m^2 \cdot s^{-2}$), according to Schindler and Mohr (2018):

$$M = \sqrt{(u'w')^2 + (v'w')^2}, \qquad \text{(Eq. 11)}$$

where u', v', and w' are the fluctuations of u, v, and w about their respective mean values following Reynold's decomposition. In each case, the form of the relationship was determined by selecting the function best fitting the data as determined using the coefficient of determination, R^2. The wind statistic accounting for the most variability in tree response at 0% severity was used consistently in statistical analysis. The collected data was processed using MATLAB (R2024a, MathWorks, Natick, MA, USA).

The experiment was designed as a one-way repeated measures analysis of covariance (ANCOVA) with one within-subject factor with five levels (pruning severity: 0%, deadwood removal, 10%, 20%, 40%) and one between-subject factor with two levels (pruning type: raised, thinned). The selected wind statistic was included as a covariate to account for the relationship between wind speed and bending moments. Pruning severity, pruning type, and their interaction were included as fixed effects, and the random effect of tree, nested within pruning treatment, was included in the statistical model. Linear mixed effects models for repeated measures ANCOVA were fit to 30-minute maximum M_B using the MIXED procedure in SAS OnDemand for Academics (SAS Institute, Inc., Cary, NC, USA).

Model variance-covariance matrix structures were examined using information criteria, and the covariance structure with the smallest Akaike Information Criterion (AIC) was selected. The Kenward-Roger correction was used to adjust the error degrees of freedom for the selected covariance structure. Equality of slopes among fixed effects were tested, and if rejected, an unequal slopes model was fit to the observations. Fixed effects were tested with the covariate set to 14 $\mathrm{m{\cdot}s^{-1}}$. For significant effects, Tukey's HSD was used to assess mean differences at three values of the covariate distributed over the upper range of the observed 30-minute maximum wind speeds (10 $\mathrm{m{\cdot}s^{-1}}$, 12.5 $\mathrm{m{\cdot}s^{-1}}$, and 15 $\mathrm{m{\cdot}s^{-1}}$).

CHAPTER 4 – RESULTS

Baseline (0% severity) data was collected from July 26 to September 14, 2023, spanning a total of 50 days. Due to a malfunctioning data acquisition system, the original experimental schedule was interrupted after collecting baseline data during the 0% severity treatment. After repairs, the schedule was modified to minimize data collection during freezing winter temperatures. Deadwood data was gathered from November 12 to November 21, 2023, over a period of 10 days. The collection of 10% data took place from November 22 to December 3, 2023, covering 12 days, while 20% data was collected between December 4 and December 11, for a duration of 8 days. Finally, 40% data was collected from December 12, 2023, to January 8, 2024, totaling 28 days.

Tree 10, assigned to the raised pruning treatment, was removed from the study shortly after the conclusion of the baseline (0% severity) period. The lowest one-third of the canopy displayed signs of rapid dieback and decline, and no longer possessed enough live foliage to be included in the study (**Figure 11**). As a result, the number of subjects representing the raised pruning category was reduced by one. All remaining trees – raised (n = 4) and thinned (n = 5) – persisted throughout the remainder of the experiment.

Figure 11 Tree 10, assigned to raised pruning treatment, removed from experiment due to declining canopy condition.

Tree Pruning

The actual severity of pruning for thinned trees was, on average, within 1.29% of the target severity. The figure reflects varying error rates depending on the severity of thinning applied: at 10% severity, the average error was 0.72% (0.65) with a minimum of 0.02% and a maximum of 1.44%; at 20% severity, it increased to 2.1% (1.64), with a minimum of 0.60% and a maximum of 3.96%; and at 40% severity, the error rate was 1.1% (1.12), with a minimum of 0.10% and a maximum of 2.68%. The greatest pruning error and variability occurred during the 20% severity, and Tree 3 had the largest margin of error among all thinned trees at each

severity: 1.44% at 10% severity, 3.96% at 20% severity, and 2.68% at 40% severity. For a comprehensive overview of the detailed error rates for each tree at every severity level, refer to Appendix B. For photographs of raised and thinned trees, see Appendices A and B, respectively.

Wind Conditions

After excluding signals contaminated by noise, 4,304 30-minute intervals were used for analysis. Wind direction remained relatively consistent throughout the experiment; however, the 40% severity trial saw a notably higher proportion of stronger wind speeds compared to all other severity windows, suggesting that more intense winds were characteristic of this trial. (**Figure 12**). The prevailing 30-minute wind direction arose from the northeast (NE) during the experiment. Instantaneous wind speeds ranged from 0.50 $\mathrm{m{\cdot}s^{-1}}$to 21.97 $\mathrm{m{\cdot}s^{-1}}$, with a maximum 30-minute mean wind speed of 9.26 $\mathrm{m{\cdot}s^{-1}}$.

The baseline period lasted 50 days and had increased modal wind direction variability with resulting wind vector angles between 0° (North) and 180° (South). After performing the deadwood severity, wind direction became less variable with vector angles between 0° (North) and 45° (East). This trend remained consistent throughout the rest of the experiment.

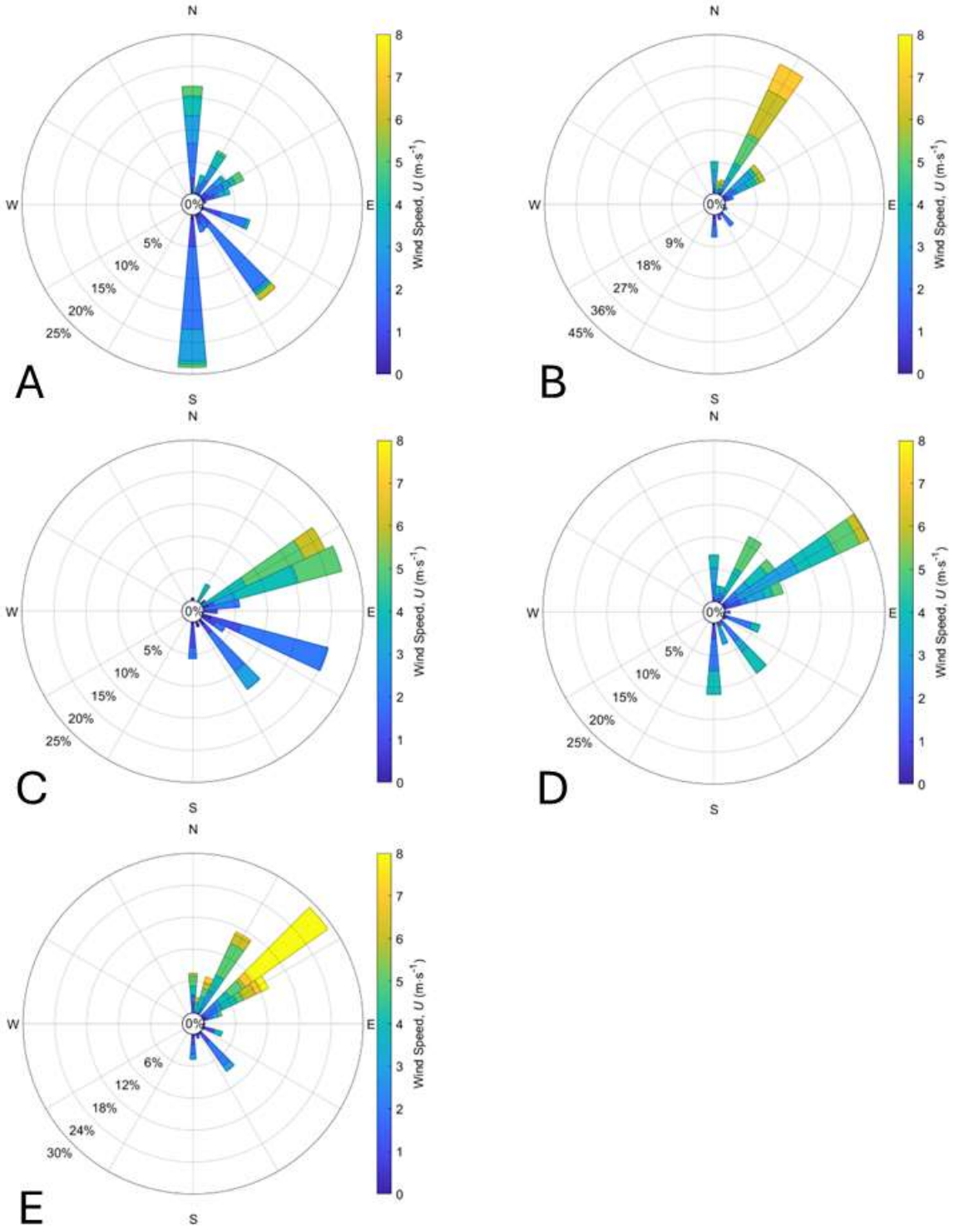

Figure 12 Wind rose showing the 30-minute resultant wind velocity at the research site for all available 30-minute intervals during each pruning severity: baseline or 0% (A), removal of deadwood (B), 10% (C), 20% (D), and 40% (E). Concentric circles represent the relative frequency of wind conditions, with spoke length depicting resultant wind directions within 36 incremental 10° bins and given wind speed denoted by color.

Pull Tests

Pull tests indicated an average tree stiffness of 3.54 GPa. Trees 2, 3, 4, 5, 8, and 9 were each calibrated through a series of four pull tests. However, due to load flucuations, Trees 1 (**Figure 13**), 6, and 7 underwent only three pull tests for calibration. The calibration coefficients (C_1), which represent the stiffness of each individual tree, are detailed in **Table *2***.

Table 2 Mean (SD) calibration coefficient, C_1 (kN·m/mm), and mean (SD) tree stiffness, E (GPa), obtained from a series of pull tests (N) conducted on individual trees.

Tree	C_1	E	N
1	82.69 (0.71)	2.99 (0.03)	3
2	29.88 (0.38)	2.32 (0.03)	4
3	41.30 (0.94)	2.99 (0.07)	4
4	85.03 (2.15)	4.73 (0.12)	4
5	64.44 (2.70)	3.95 (0.17)	4
6	64.30 (0.38)	4.47 (0.03)	3
7	90.44 (2.44)	4.08 (0.11)	3
8	24.64 (0.66)	2.19 (0.06)	4
9	103.20 (0.85)	4.21 (0.03)	4

Bivariate Model Selection

In the analysis, goodness of fit tests indicated that the most appropriate bivariate model depicting the relationship between wind conditions and tree wind loads was maximum u and maximum M_B for both pruning treatments (**Table 3**). A positive quadratic function best described the relationship between the two variables at each severity, resulting in the largest R^2 value when compared to exponential, linear, logarithmic, polynomial, and power function transformations.

Table 3 Goodness of fit tests used for selecting the bivariate model of 30-minute u and M_B. Models included maximum u and maximum streamwise M_B (Maximum u), mean u and mean streamwise M_B (Mean u), maximum $|\boldsymbol{u}|$ and maximum resultant M_B(Maximum $|\boldsymbol{u}|$), mean $|\boldsymbol{u}|$ and mean resultant M_B (Mean $|\boldsymbol{u}|$), maximum M and maximum streamwise M_B (Maximum M), and mean M and mean streamwise M_B (Mean M). Trees are grouped by treatment (raised or thinned).

	Coefficient of Determination (R^2)
Bivariate Model	**0 % Severity**
Raised Treatment	
Maximum u	**0.54**
Mean u	0.19
Maximum $\|\boldsymbol{u}\|$	0.52
Mean $\|\boldsymbol{u}\|$	0.19
Maximum M	0.52
Mean M	0.38
Thinned Treatment	
Maximum u	**0.72**
Mean u	0.18
Maximum $\|\boldsymbol{u}\|$	0.7
Mean $\|\boldsymbol{u}\|$	0.25
Maximum M	0.66
Mean M	0.64

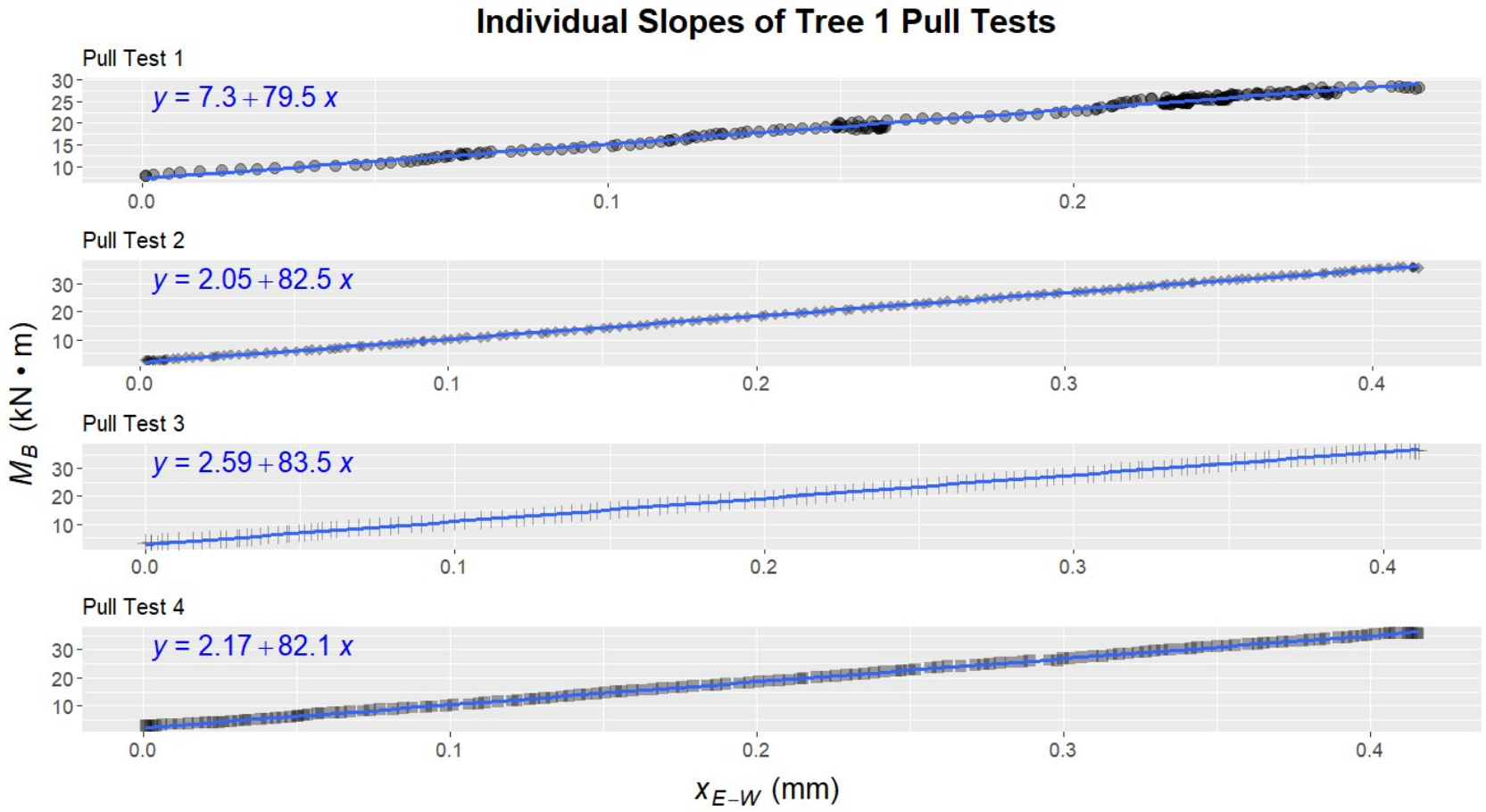

Figure 13 The slope of an ordinary least-squares regression line given the average of the series of pull tests for each tree and fit to model M_B as a function of x_{E-W} (Eq. 4). Pull tests that resulted in nonlinear data were removed from the final calculation of C_1. For example, pull test 1 was removed from the final average of the series of pull tests for Tree 1, leaving pull test 2, 3, 4.

Wind-Induced Bending Moments

In total, 4,304 observations of 30-minute maximum wind speed and 30-minute maximum bending moments were obtained from all the available 30-minute intervals in the study. Individual scatter plots (**Figure 14**) revealed a curvilinear relationship between 30-minute maximum u and 30-minute maximum streamwise M_B at each of the five pruning severities (see Appendix C). Figures 15 and 16 display all severity levels on a single split plot divided by raised and thinned pruning treatments. **Figure 15** presents the data without individual data points, while **Figure 16** includes the data points for a more detailed representation.

Twenty-three covariance structures with varying parameters were examined. Among these covariance structures, the AIC fit index indicated that first-order autoregressive [ar(1)] best fit the dataset. Statistical inferences were made with the covariate set to 14 $\mathrm{m{\cdot}s^{-1}}$ (u^2 = 196 $\mathrm{m{\cdot}s^{-1}}$) to represent a value towards the upper limit of the observed maximum wind speeds. The one-way repeated measures ANCOVA revealed that 30-minute maximum bending moments did not differ between pruning treatments (F = 2.62, p = 0.14), but 30-minute maximum M_B varied significantly among pruning severities (F = 7.09, p < 0.0001) (**Table 4**).

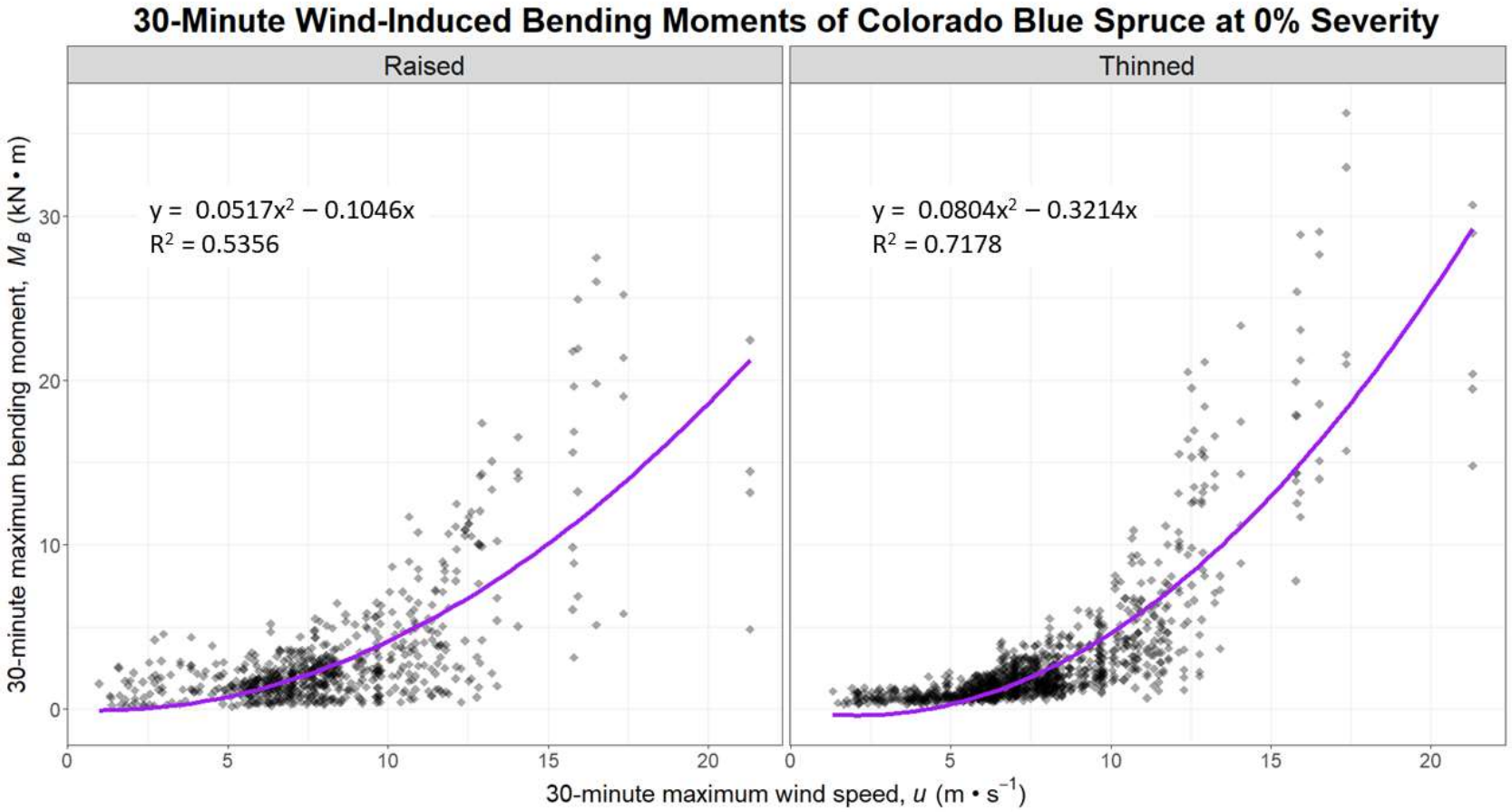

Figure 14 Split plot scatter plot of raised (left) and thinned (right) *Picea pungens*, showing best fit lines of 30-minute maximum streamwise bending moment, M_B (kN·m), against 30-minute maximum streamwise wind speed, u (m·s^{-1}) at 0% severity (diamond marker, solid purple line).

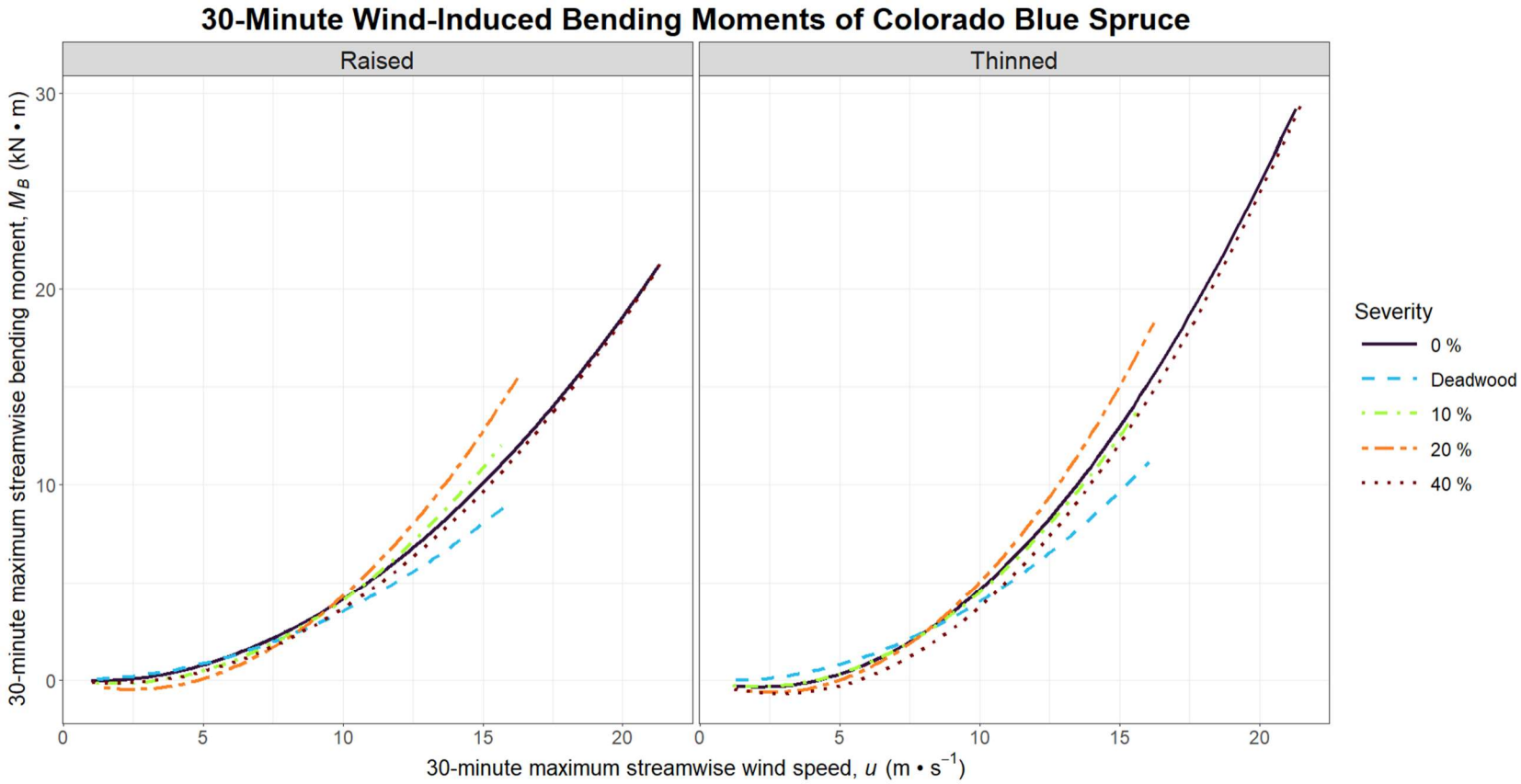

Figure 15 Positive quadratic functions showing trends between 30-minute maximum u and 30-minute maximum streamwise M_B at each of the five pruning severities separated by pruning treatment. Individual data points have been removed for clarity.

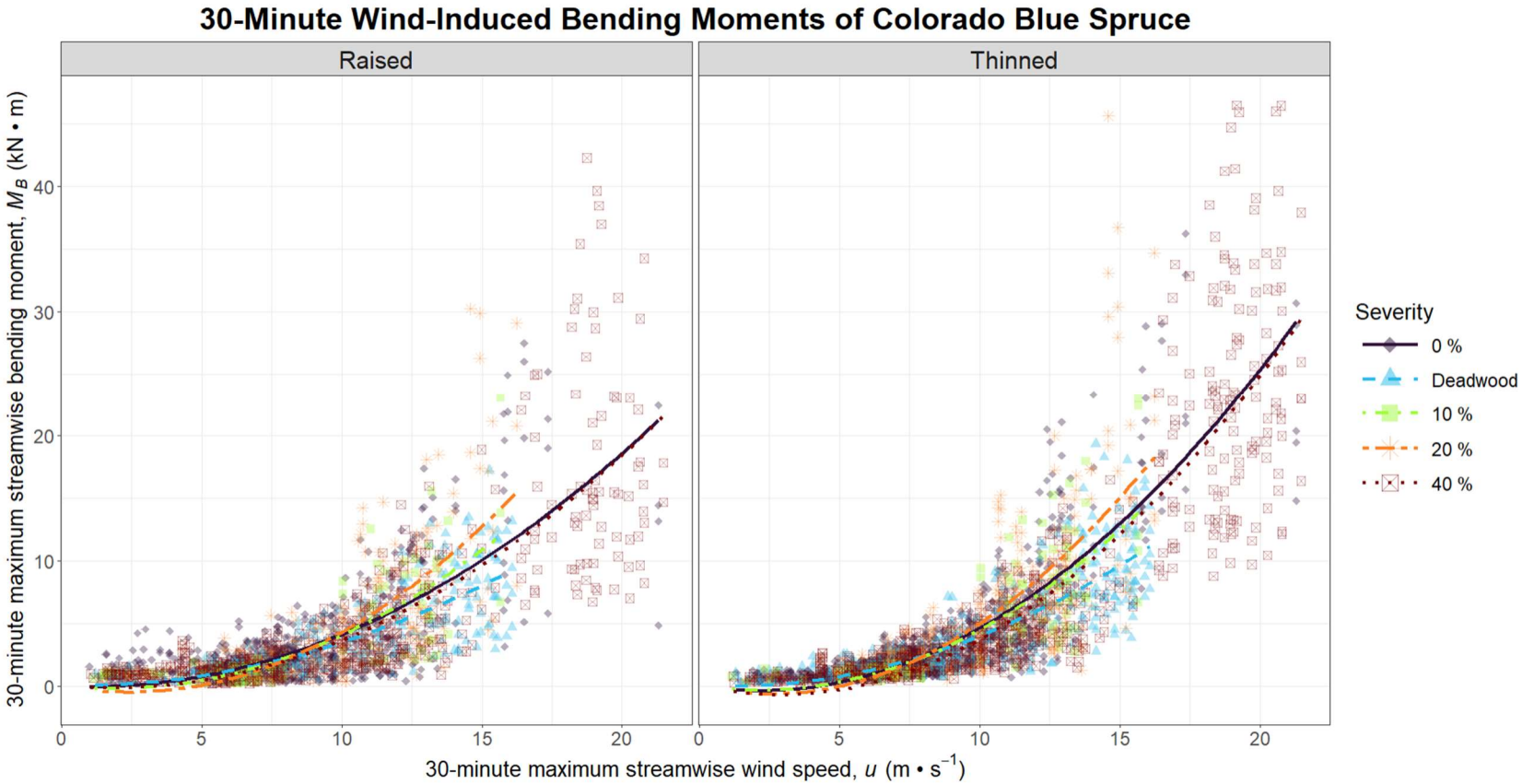

Figure 16 Positive quadratic functions showing curvilinear relationship between 30-minute maximum u and 30-minute maximum streamwise M_B at each of the five pruning severities separated by pruning treatment. Data points have been included for detailed representation of this relationship.

Table 4 ANCOVA table with the covariate set at 14 $\mathrm{m{\cdot}s^{-1}}$. *** indicates statistical significance, with α = 0.05.

Effect	Num DF	Den DF	F value	p value
Treatment	1	8.33	2.62	0.1424
Severity	4	1372.00	7.09	< 0.0001***
Treatment*Severity	4	1372.00	1.45	0.2141
u^2*Treatment*Severity	10	3096.00	499.22	< 0.0001***

Mean separation (**Figure 17**) was conducted at three winds chosen to represent the upper range of 30-minute maximum u experienced during all severity periods: 10 $\mathrm{m{\cdot}s^{-1}}$, 12.5 $\mathrm{m{\cdot}s^{-1}}$, and 15 $\mathrm{m{\cdot}s^{-1}}$. Wind speeds greater than 15 $\mathrm{m{\cdot}s^{-1}}$ were experienced during the 0% and 40% severity periods, but these speeds were not recorded during the other severity windows and did not provide meaningful comparisons to severity periods that did not experience these greater wind speeds. Compared to the other severities, the average 30-minute maximum M_B was significantly lower with deadwood removed at the two higher wind speeds (12.5 and 15 $\mathrm{m{\cdot}s^{-1}}$). At the lowest wind speed (10 $\mathrm{m{\cdot}s^{-1}}$), the average 30-minute maximum M_B after deadwood removal was significantly less than 20% severity, but there were no differences in wind loads among other severities.

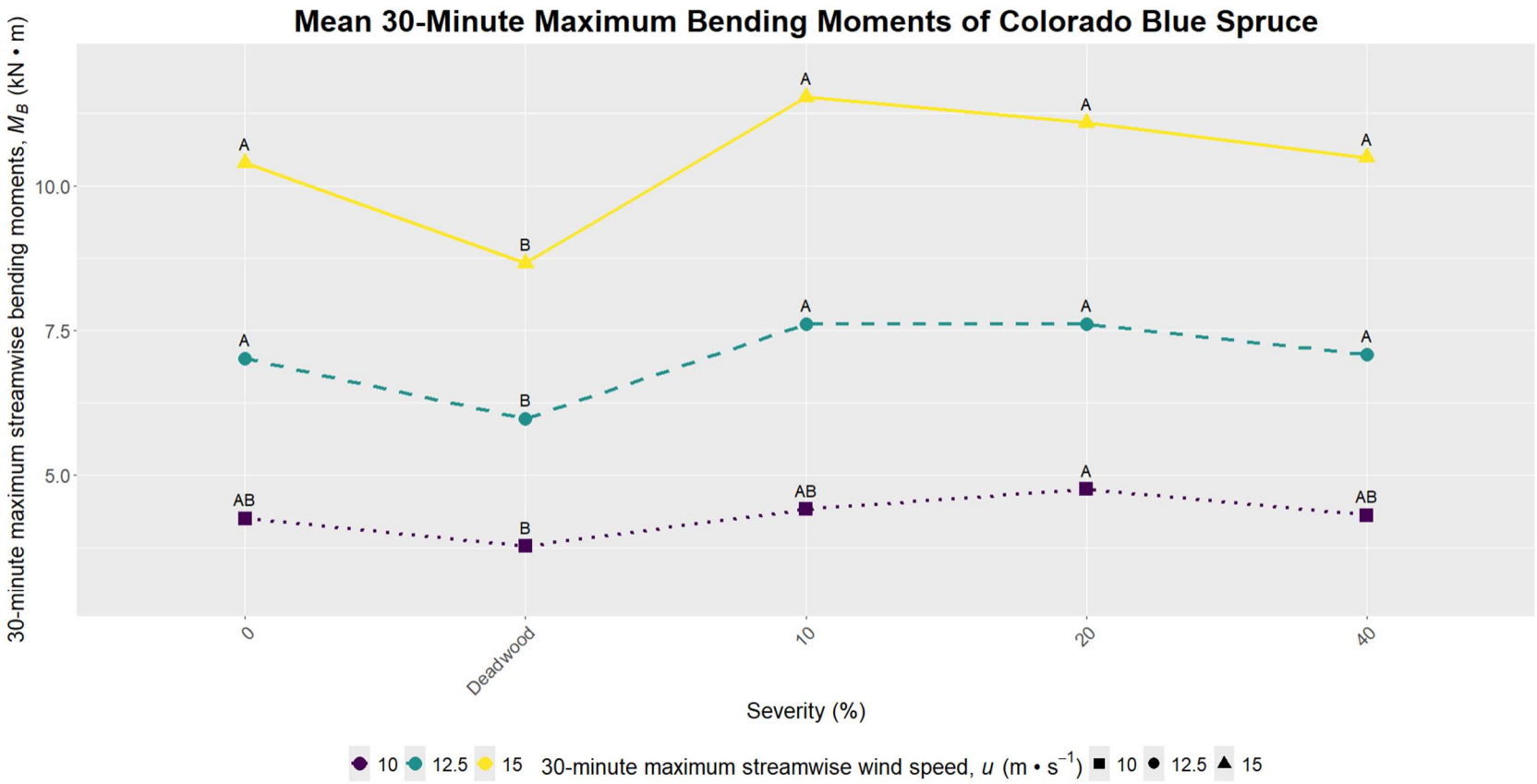

Figure 17 Mean separation of 30-minute maximum bending moments of *P. pungens* at three different covariate values. Means followed by the same letter are not significantly different at alpha = 0.05.

CHAPTER 5 – DISCUSSION

The primary objective of this study was to evaluate the effects of pruning type and severity on the wind-induced bending moments of Colorado blue spruce, with the ultimate aim of providing actionable recommendations for pruning strategies to mitigate wind-induced failures. Our findings highlight the critical role of deadwood removal in enhancing tree stability, as its removal was associated with reduced drag and bending moments during high winds. This result underscores the importance of deadwood management for improving wind resistance, suggesting that targeted pruning strategies focused on deadwood could significantly reduce wind load-induced risks for mature trees in urban environments.

While no previous research has specifically examined the impact of deadwood removal on wind-induced bending moments in urban trees, our findings align with broader studies on tree stability and wind resistance. Studies by Kane and James (2011), Pavlis et al. (2008), and Smiley and Kane (2006) highlight that reducing mass can lower wind loads, supporting our finding that deadwood removal reduces wind-induced forces. However, our study uniquely discovered that sequential pruning, which removes additional biomass beyond deadwood, did not have the same effect on wind loading. This suggests that the rigidity of deadwood plays a crucial role in how trees interact with wind forces, differing from the flexible, living tissue in healthy trees, which helps dissipate wind energy through movement (James, 2003). Our results further contribute to the understanding that deadwood's inflexibility may increase stress concentrations on the tree, exacerbating the risk of structural damage under wind loads.

One of the novel findings of our study is the significant impact of deadwood on wind-induced bending moments, which had not been directly addressed in previous urban tree pruning studies. We identified that deadwood's rigidity potentially impairs the tree's ability to bend and sway, concentrating stress at specific points and increasing the likelihood of failure. Deadwood accumulation also alters the tree's dynamic properties, affecting its natural sway frequency and aerodynamic damping, which can result in resonant oscillations that amplify tree movement and heighten the risk of structural failure (Peltola et al., 2013). Additionally, deadwood disrupts mass distribution, leading to imbalances that can further affect the tree's sway dynamics and overall structural integrity (Stathers et al., 1994).

Interestingly, our study also challenges conventional pruning practices. While much of the literature emphasizes removing leaf and branch mass to reduce wind drag (Angelou et al., 2019), we found that deadwood removal had a more substantial effect on wind loading in large spruce trees. This suggests that urban forestry management should reconsider current pruning priorities, placing more emphasis on deadwood management of Colorado blue spruce and other tree species that tend to retain and accumulate deadwood as they mature.

Moreover, we observed that raising trees did not increase their vulnerability to wind-induced failure, contrary to traditional expectations. This surprising result suggests that the relationship between pruning practices, tree morphology, and wind resistance is more complex than previously understood, particularly for large, mature trees like Colorado blue spruce.

Several limitations of this study must be addressed. First, the experiments were conducted under relatively low wind conditions (resulting in bending moments below 5 kN·m), limiting our ability to extrapolate results to extreme wind events. Furthermore, no significant

impact was found from branch removal location on wind-induced bending moments, which challenges prior studies that have linked pruning type and severity to wind resistance (Burcham et al., 2020, 2021). The lack of detailed mass measurements for removed branches also complicates our interpretation, as a more thorough analysis of branch characteristics would enhance our understanding of deadwood's role in wind resistance. Additionally, not measuring the amount of deadwood removed from the trees further limits our understanding of how deadwood reduction might influence wind resistance, as the mass and distribution of the remaining deadwood could have played a significant role in the observed results.

Environmental factors may have influenced the results. The presence of a row of ponderosa pine to the east of the spruce trees may have shielded the subject trees from prevailing winds, reducing wind exposure and potentially affecting the observed bending moments. Additionally, the proximity of neighboring spruce trees may have introduced mutual shielding, where wind is redirected by adjacent trees, thus impacting the results.

Our study suggests that urban forestry management should prioritize deadwood removal as a key strategy for enhancing tree stability, particularly in species prone to deadwood accumulation, such as Colorado blue spruce. These findings have practical implications for urban tree maintenance, offering insights into how pruning strategies can be optimized to mitigate wind-induced failures in mature trees. Moreover, the unexpected results regarding tree raising and the role of deadwood challenge current urban tree management practices and suggest that a more nuanced approach to pruning may be needed.

Future research should further explore the role of deadwood in wind dynamics, particularly in urban environments, to develop more effective management strategies. By

addressing gaps in the understanding of tree biomechanics and pruning impacts, we can improve the resilience and sustainability of urban forests, contributing to healthier ecosystems better equipped to withstand the challenges posed by changing environmental conditions.

CHAPTER 6 – CONCLUSION

This study offers valuable insights into the effects of pruning on wind-induced bending moments in large, open-grown evergreens within a moderate wind environment. While the trees experienced higher wind speeds than those recorded in similar studies (Burcham et al., 2020, 2021), the wind loads remained mild and non-destructive. Future research should explore pruning effects in regions with strong, dynamic wind conditions that are more likely to cause tree damage. The findings contribute to existing literature on deciduous species and provide novel guidance for the pruning of large evergreens. Notably, the removal of deadwood emerged as the most effective method for reducing wind loads on Colorado blue spruce at all tested velocities, while pruning thinned trees did not significantly alter canopy shape or reduce drag. Although previous studies have suggested that changes in mass influence wind loading more than canopy shape, the raised trees in this study demonstrated that removing lower canopy branches allowed wind to pass freely beneath the remaining foliage. Future investigations should focus on mature, solitary trees to accurately represent open-grown specimens and incorporate a broader range of mechanical metrics to elucidate the complex interactions between trees and wind. As urban greenspaces and canopy cover become increasingly vital for sustainable environments, understanding how pruning affects tree health and stability is essential. Despite extensive research on deciduous trees, knowledge gaps remain regarding evergreens, warranting continued study of the short- and long-term impacts of pruning. Such research will enhance urban forest management practices, ensuring the longevity and structural integrity of evergreen trees in changing environmental conditions.

BIBLIOGRAPHY

American National Standards Institute (ANSI). (2023). *American National Standard for Tree Care Operations for trees, shrubs, palms, and other woody landscape plants—ANSI A300 Clause 5: Pruning*. Tree Care Industry Association.

Angelou, N., Dellwik, E., & Mann, J. (2019). Wind load estimation on an open-grown European oak tree. *Forestry: An International Journal of Forest Research*, *92*(4), 381–392. https://doi.org/10.1093/forestry/cpz026

Archer, R. R. (2013). *Growth Stresses and Strains in Trees*. Springer Science & Business Media.

Baker, C. J. (1997). Measurements of the natural frequencies of trees. *Journal of Experimental Botany*, *48*(5), 1125–1132. https://doi.org/10.1093/jxb/48.5.1125

Bargali, S. S., Padalia, K., & Bargali, K. (2019). Effects of tree fostering on soil health and microbial biomass under different land use systems in the Central Himalayas. *Land Degradation & Development*, *30*(16), 1984–1998. https://doi.org/10.1002/ldr.3394

Barrios, E., Valencia, V., Jonsson, M., Brauman, A., Hairiah, K., Mortimer, P. E., & Okubo, S. (2018). Contribution of trees to the conservation of biodiversity and ecosystem services in agricultural landscapes. *International Journal of Biodiversity Science, Ecosystem Services & Management*, *14*(1), 1–16. https://doi.org/10.1080/21513732.2017.1399167

Blackburn, P., Petty, J. A., & Miller, K. F. (1988). An Assessment of the Static and Dynamic Factors Involved in Windthrow. *Forestry: An International Journal of Forest Research*, *61*(1), 29–43. https://doi.org/10.1093/forestry/61.1.29

Brudi, E. (2002). Trees and Statics: An Introduction. *Arborist News*, *11*(4), 28–33.

Burcham, D. C., Autio, W. R., James, K., Modarres-Sadeghi, Y., & Kane, B. (2020). Effect of pruning type and severity on vibration properties and mass of Senegal mahogany (Khaya senegalensis) and rain tree (Samanea saman). *Trees*, *34*(1), 213–228. https://doi.org/10.1007/s00468-019-01912-8

Burcham, D. C., Autio, W. R., Modarres-Sadeghi, Y., & Kane, B. (2021). After pruning, wind-induced bending moments and vibration decrease more on reduced than raised Senegal mahogany (Khaya senegalensis). *Urban Forestry & Urban Greening*, *61*, 127100. https://doi.org/10.1016/j.ufug.2021.127100

Cariñanos, P., Calaza-Martínez, P., O'Brien, L., & Calfapietra, C. (2017). The Cost of Greening: Disservices of Urban Trees. In D. Pearlmutter, C. Calfapietra, R. Samson, L. O'Brien, S. Krajter Ostoić, G. Sanesi, & R. Alonso del Amo (Eds.), *The Urban Forest: Cultivating Green Infrastructure for People and the Environment* (pp. 79–87). Springer International Publishing. https://doi.org/10.1007/978-3-319-50280-9_9

Chauhan, S. K., Singh, S., Sharma, S., Vashist, B. B., Sharma, R., & Saralch, H. S. (2018). Soil health (physical, chemical and biological) status under short rotation tree plantations on riverain soils. *Journal of Pharmacognosy and Phytochemistry*, *7*(5), 1599–1605.

Clair, B., Fournier, M., Prevost, M. F., Beauchene, J., & Bardet, S. (2003). Biomechanics of buttressed trees: Bending strains and stresses. *American Journal of Botany*, *90*(9), 1349–1356. https://doi.org/10.3732/ajb.90.9.1349

Clapp, J. C., Ryan III, H. D. P., Harper, R. W., & Bloniarz, D. V. (2014). Rationale for the increased use of conifers as functional green infrastructure: A literature review and synthesis. *Arboricultural Journal*, *36*(3), 161–178. https://doi.org/10.1080/03071375.2014.950861

Colorado Climate Center—Colorado's Climate. (n.d.). Retrieved November 30, 2023, from https://climate.colostate.edu/climate_long.html

Conway, T. M., & Yip, V. (2016). Assessing residents' reactions to urban forest disservices: A case study of a major storm event. *Landscape and Urban Planning*, *153*, 1–10. https://doi.org/10.1016/j.landurbplan.2016.04.016

Davies, H. J., Doick, K. J., Hudson, M. D., & Schreckenberg, K. (2017). Challenges for tree officers to enhance the provision of regulating ecosystem services from urban forests. *Environmental Research*, *156*, 97–107. https://doi.org/10.1016/j.envres.2017.03.020

de Langre, E. (2019). Plant vibrations at all scales: A review. *Journal of Experimental Botany*, *70*(14), 3521–3531. https://doi.org/10.1093/jxb/erz209

Delshammar, T., Ostberg, J., & O¨xell, C. (2015). Urban trees and ecosystem disservices—A pilot study using complaints records from three Swedish cities. *Arboriculture and Urban Forestry*, *41*, 187–193.

Elmendorf, W. (2008). The Importance of Trees and Nature in Community: A Review of the Relative Literature. *Arboriculture & Urban Forestry*, *34*(3), 152–156. https://doi.org/10.48044/jauf.2008.020

Endreny, T. A. (2018). Strategically growing the urban forest will improve our world. *Nature Communications*, *9*(1), 1160. https://doi.org/10.1038/s41467-018-03622-0

Endreny, T., Santagata, R., Perna, A., Stefano, C. D., Rallo, R. F., & Ulgiati, S. (2017). Implementing and managing urban forests: A much needed conservation strategy to increase ecosystem services and urban wellbeing. *Ecological Modelling*, *360*, 328–335. https://doi.org/10.1016/j.ecolmodel.2017.07.016

Ennos, A. R. (1997). Wind as an ecological factor. *Trends in Ecology & Evolution*, *12*(3), 108–111. https://doi.org/10.1016/S0169-5347(96)10066-5

Flesch, T. K., & Wilson, J. D. (1999). Wind and remnant tree sway in forest cutblocks. II. Relating measured tree sway to wind statistics. *Agricultural and Forest Meteorology*, *93*(4), 243–258. https://doi.org/10.1016/S0168-1923(98)00113-0

Fraser, A. (1962). Wind Tunnel Studies of the Forces Acting on the Crowns of Small Trees. *Forestry Commission*, 178–183.

Gardiner, B. A. (1995). The interactions of wind and tree movement in forest canopies. *Wind and Trees*, 41–59. https://doi.org/10.1017/cbo9780511600425.003

Gardiner, B., & Quine, C. (2000). The mechanical adaption of tree to environmental influences. *Proceedings of 3rd Plant Biomechanics Conference*, 71–82.

Gilman, E., Grabosky, J., Jones, S., & Harchick, C. (2008a). Effects of Pruning Dose and Type on Trunk Movement in Tropical Storm Winds. *Arboriculture and Urban Forestry*, *34*. https://doi.org/10.48044/jauf.2008.003

Gilman, E., Masters, F., & Grabosky, J. (2008b). Pruning Affects Tree Movement in Hurricane Force Wind. *Arboriculture & Urban Forestry*, *34*(1), 20–28. https://doi.org/10.48044/jauf.2008.004

Guitard, D. G. E., & Castera, P. (1995). Experimental analysis and mechanical modelling of windinduced tree sways. In J. Grace & M. P. Coutts (Eds.), *Wind and Trees* (pp. 182–194). Cambridge University Press. https://doi.org/10.1017/CBO9780511600425.010

Hamzah, H., Othman, N., Badrulhisham, N., & Karlinasari, L. (2021). Pruning Urban Trees without Skill: An act of unintentional vandalism. *Asian Journal of Environment-Behaviour Studies*, *6*(20), Article 20. https://doi.org/10.21834/ajebs.v6i20.397

Hansen, W. R., Chronic, B. J., & Matelock, J. (1978). Climatography of the Front Range Urban Corridor and Vicinity, Colorado. In *Professional Paper* (No. 1019). U.S. Geological Survey. https://doi.org/10.3133/pp1019

Hassinen, A., Lemettinen, M., Peltola, H., Kellomäki, S., & Gardiner, B. (1998). A prism-based system for monitoring the swaying of trees under wind loading. *Agricultural and Forest Meteorology*, *90*(3), 187–194. https://doi.org/10.1016/S0168-1923(98)00052-5

Huang, Y.-S., Hsu, F.-L., Lee, C.-M., & Juang, J.-Y. (2017). Failure mechanism of hollow tree trunks due to cross-sectional flattening. *Royal Society Open Science*, *4*(4), 160972. https://doi.org/10.1098/rsos.160972

James, K. (2003). Dynamic Loading of Trees. *Arboriculture & Urban Forestry (AUF)*, *29*(3), 165–171. https://doi.org/10.48044/jauf.2003.020

James, K. R., & Kane, B. (2008). Precision digital instruments to measure dynamic wind loads on trees during storms. *Agricultural and Forest Meteorology*, *148*(6), 1055–1061. https://doi.org/10.1016/j.agrformet.2008.02.003

Kane, B. (2014). Determining parameters related to the likelihood of failure of red oak (Quercus rubra L.) from winching tests. *Trees*, *28*(6), 1667–1677. https://doi.org/10.1007/s00468-014-1076-0

Kane, B., & James, K. R. (2011). Dynamic properties of open-grown deciduous trees. *Canadian Journal of Forest Research*, *41*(2), 321–330. https://doi.org/10.1139/X10-211

Kane, B., Modarres-Sadeghi, Y., James, K. R., & Reiland, M. (2014). Effects of crown structure on the sway characteristics of large decurrent trees. *Trees*, *28*(1), 151–159. https://doi.org/10.1007/s00468-013-0938-1

Karlovich, D., Groninger, J., & Close, D. (2000). Tree Condition Associated with Topping in Southern Illinois Communities. *Arboriculture & Urban Forestry*, *26*(2), 87–91. https://doi.org/10.48044/jauf.2000.010

Kerzenmacher, T., & Gardiner, B. (1998). A mathematical model to describe the dynamic response of a spruce tree to the wind. *Trees*, *12*(6), 385–394. https://doi.org/10.1007/s004680050165

Koeser, A. K., & Smiley, E. T. (2017). Impact of assessor on tree risk assessment ratings and prescribed mitigation measures. *Urban Forestry & Urban Greening*, *24*, 109–115. https://doi.org/10.1016/j.ufug.2017.03.027

Lilly, S. J. (2001). *Arborists' Certification Study Guide*. International Society of Arboriculture.

Lilly, S. J., Gilman, E. F., & Smiley, E. T. (2019). *Best Management Practices—Pruning, 3rd Edition* (3rd ed.).

Ma, B., Hauer, R. J., Wei, H., Koeser, A. K., Peterson, W., Simons, K., Timilsina, N., Werner, L. P., & Xu, C. (2020). An Assessment of Street Tree Diversity: Findings and Implications in the United States. *Urban Forestry & Urban Greening*, *56*, 126826. https://doi.org/10.1016/j.ufug.2020.126826

Mattheck, C., & Breloer, H. (1994). The body language of trees: A handbook for failure analysis. *The Body Language of Trees: A Handbook for Failure Analysis.* https://www.cabdirect.org/cabdirect/abstract/19960600908

Mayer, H. (1987). Wind-induced tree sways. *Trees*, *1*(4), 195–206. https://doi.org/10.1007/BF01816816

Milne, R. (1991). Dynamics of swaying of Picea sitchensis. *Tree Physiology*, *9*(3), 383–399. https://doi.org/10.1093/treephys/9.3.383

Moore, J. R. (2000). Differences in maximum resistive bending moments of Pinus radiata trees grown on a range of soil types. *Forest Ecology and Management*, *135*(1), 63–71. https://doi.org/10.1016/S0378-1127(00)00298-X

Moore, J. R., & Maguire, D. A. (2005). Natural sway frequencies and damping ratios of trees: Influence of crown structure. *Trees*, *19*(4), 363–373. https://doi.org/10.1007/s00468-004-0387-y

Mortimer, M. J., & Kane, B. (2004). Hazard tree liability in the United States: Uncertain risks for owners and professionals. *Urban Forestry & Urban Greening*, *2*(3), 159–165. https://doi.org/10.1078/1618-8667-00032

Murphy, T. N., Henson, M., & Vanclay, J. K. (2005). Growth stress in *Eucalyptus dunnii*. *Australian Forestry*, *68*(2), 144–149. https://doi.org/10.1080/00049158.2005.10674958

Neild, S. A., & Wood, C. J. (1999). Estimating stem and root-anchorage flexibility in trees. *Tree Physiology*, *19*(3), 141–151. https://doi.org/10.1093/treephys/19.3.141

NOAA NCEI U.S. Climate Normals Quick Access. (n.d.). Retrieved December 5, 2023, from https://www.ncei.noaa.gov/access/us-climate-normals/#dataset=normals-annualseasonal&timeframe=30&location=CO&station=US1COLR0284

Norris, M. (2007). *Tree Risk Assessments – What Works – What Does Not – Can We Tell? A review of a range of existing tree risk assessment methods*. 1–31.

Nowak, D. J., Crane, D. E., & Stevens, J. C. (2006). Air pollution removal by urban trees and shrubs in the United States. *Urban Forestry & Urban Greening*, *4*(3), 115–123. https://doi.org/10.1016/j.ufug.2006.01.007

Oliver, H. R., & Mayhead, G. J. (1974). Wind Measurements in a Pine Forest During a Destructive Gale. *Forestry: An International Journal of Forest Research*, *47*(2), 185–194. https://doi.org/10.1093/forestry/47.2.185

Pavlis, M., Kane, B., Harris, J., & Seiler, J. (2008). The Effects of Pruning on Drag and Bending Moment of Shade Trees. *Arboric Urb For*, *34*. https://doi.org/10.48044/jauf.2008.028

Peltola, H. (1996). Swaying of trees in response to wind and thinning in a stand of Scots pine. *Boundary-Layer Meteorology*, *77*(3), 285–304. https://doi.org/10.1007/BF00123529

Peltola, H., Gardiner, B., & Nicoll, B. (2013). Mechanics of wind damage. *Agric For Meteorol*, *151*, 328–344.

Peltola, H., Kellomäki, S., Hassinen, A., & Granander, M. (2000). Mechanical stability of Scots pine, Norway spruce and birch: An analysis of tree-pulling experiments in Finland. *Forest Ecology and Management*, *135*(1), 143–153. https://doi.org/10.1016/S0378-1127(00)00306-6

Peltola, H., Kellomäki, S., Väisänen, H., & Ikonen, V.-P. (1999). A mechanistic model for assessing the risk of wind and snow damage to single trees and stands of Scots pine, Norway spruce, and birch. *Canadian Journal of Forest Research*, *29*(6), 647–661. https://doi.org/10.1139/x99-029

Pramova, E., Locatelli, B., Djoudi, H., & Somorin, O. A. (2012). Forests and trees for social adaptation to climate variability and change. *WIREs Climate Change*, *3*(6), 581–596. https://doi.org/10.1002/wcc.195

Roodbaraky, H. J., Baker, C. J., Dawson, A. R., & Wright, C. J. (1994). Experimental observations of the aerodynamic characteristics of urban trees. *Journal of Wind Engineering and Industrial Aerodynamics*, *52*, 171–184. https://doi.org/10.1016/0167-6105(94)90046-9

Rottmann, M. (1985). *Snow damage in coniferous forests. Contributions to the assessment of the risk of snow damage, damage prevention and treatment of snow-damaged coniferous forests.* 159.

Rudnicki, M., Mitchell, S. J., & Novak, M. D. (2004). Wind tunnel measurements of crown streamlining and drag relationships for three conifer species. *Canadian Journal of Forest Research*, *34*(3), 666–676. https://doi.org/10.1139/x03-233

Rudnicki, M., Silins, U., Lieffers, V. J., & Josi, G. (2001). Measure of simultaneous tree sways and estimation of crown interactions among a group of trees. *Trees*, *15*(2), 83–90. https://doi.org/10.1007/s004680000080

Salbitano, F., Borelli, S., Conigliaro, M., & Chen, Y. (with FAO). (2016). *Guidelines on urban and peri-urban forestry*. Food and Agriculture Organization of the United Nations.

Salmond, J. A., Tadaki, M., Vardoulakis, S., Arbuthnott, K., Coutts, A., Demuzere, M., Dirks, K. N., Heaviside, C., Lim, S., Macintyre, H., McInnes, R. N., & Wheeler, B. W. (2016). Health and climate related ecosystem services provided by street trees in the urban environment. *Environmental Health*, *15*(1), S36. https://doi.org/10.1186/s12940-016-0103-6

Sander, H., Polasky, S., & Haight, R. G. (2010). The value of urban tree cover: A hedonic property price model in Ramsey and Dakota Counties, Minnesota, USA. *Ecological Economics*, *69*(8), 1646–1656. https://doi.org/10.1016/j.ecolecon.2010.03.011

Schindler, D. (2008). Responses of Scots pine trees to dynamic wind loading. *Agricultural and Forest Meteorology*, *148*(11), 1733–1742. https://doi.org/10.1016/j.agrformet.2008.06.003

Schindler, D., & Mohr, M. (2018). Non-oscillatory response to wind loading dominates movement of Scots pine trees. *Agricultural and Forest Meteorology*, *250–251*, 209–216. https://doi.org/10.1016/j.agrformet.2017.12.258

Schmidlin, T. W. (2009). Human fatalities from wind-related tree failures in the United States, 1995–2007. *Natural Hazards*, *50*(1), 13–25. https://doi.org/10.1007/s11069-008-9314-7

Silins, U., Lieffers, V. J., & Bach, L. (2000). The effect of temperature on mechanical properties of standing lodgepole pine trees. *Trees*, *14*(8), 424–428. https://doi.org/10.1007/s004680000065

Smiley, E., & Kane, B. (2006). The Effects of Pruning Type on Wind Loading of Acer rubrum. *Canadian Journal of Forest Research*, *36*, 1951–1958. https://doi.org/10.1139/x06-086

Smiley, E., Matheny, N., & Lilly, S. (2017). *Tree Risk Assessment* (2nd ed.). International Society of Arboriculture.

Stathers, R. J., Rollerson, T. P., & Mitchell, S. J. (1994). *Windthrow handbook for British Columbia forests. Research program working paper No. 9401* (No. MIC-94-07589/XAB). No corporate text available. https://www.osti.gov/biblio/6549909

Stewart, M. G., O'Callaghan, D., & Hartley, M. (2013). Review of QTRA and Risk-based Cost-benefit Assessment of Tree Management. *Arboriculture & Urban Forestry (AUF)*, *39*(4), 165–172. https://doi.org/10.48044/jauf.2013.022

Suchocka, M., Swoczyna, T., Kosno-Jończy, J., & Kalaji, H. M. (2021). Impact of heavy pruning on development and photosynthesis of Tilia cordata Mill. Trees. *PLOS ONE*, *16*(8), e0256465. https://doi.org/10.1371/journal.pone.0256465

TCIA. (2017). *American National Standard for Tree Care Operations—Tree, Shrub, and Other Woody Plant Management—Standard Practices (Pruning)*. Tree Care Industry Association, Inc., Londonderry, NH, USA.

Threlfall, C. G., Mata, L., Mackie, J. A., Hahs, A. K., Stork, N. E., Williams, N. S. G., & Livesley, S. J. (2017). Increasing biodiversity in urban green spaces through simple vegetation interventions. *Journal of Applied Ecology*, *54*(6), 1874–1883. https://doi.org/10.1111/1365-2664.12876

Turner-Skoff, J. B., & Cavender, N. (2019). The benefits of trees for livable and sustainable communities. *PLANTS, PEOPLE, PLANET*, *1*(4), 323–335. https://doi.org/10.1002/ppp3.39

Tzoulas, K., Korpela, K., Venn, S., Yli-Pelkonen, V., Kaźmierczak, A., Niemela, J., & James, P. (2007). Promoting ecosystem and human health in urban areas using Green Infrastructure: A literature review. *Landscape and Urban Planning*, *81*(3), 167–178. https://doi.org/10.1016/j.landurbplan.2007.02.001

United Nations. (2015). *Transforming our World: The 2030 Agenda for Sustainable Development*. https://sdgs.un.org/publications/transforming-our-world-2030-agenda-sustainable-development-17981

Vollsinger, S., Mitchell, S. J., Byrne, K. E., Novak, M. D., & Rudnicki, M. (2005). Wind tunnel measurements of crown streamlining and drag relationships for several hardwood species. *Canadian Journal of Forest Research*, *35*(5), 1238–1249. https://doi.org/10.1139/x05-051

Watson, A. (2000). Wind-induced forces in the near-surface lateral roots of radiata pine. *Forest Ecology and Management*, *135*(1), 133–142. https://doi.org/10.1016/S0378-1127(00)00305-4

Wellpott, A. (2008). *Stability of continuous cover forests*. https://era.ed.ac.uk/handle/1842/11534

Zobel, B. J., & van Buijtenen, J. P. (1989). Wood Variation and Wood Properties. In B. J. Zobel & J. P. van Buijtenen (Eds.), *Wood Variation: Its Causes and Control* (pp. 1–32). Springer. https://doi.org/10.1007/978-3-642-74069-5_

APPENDIX A – RAISED TREATMENT PHOTOGRAPHS

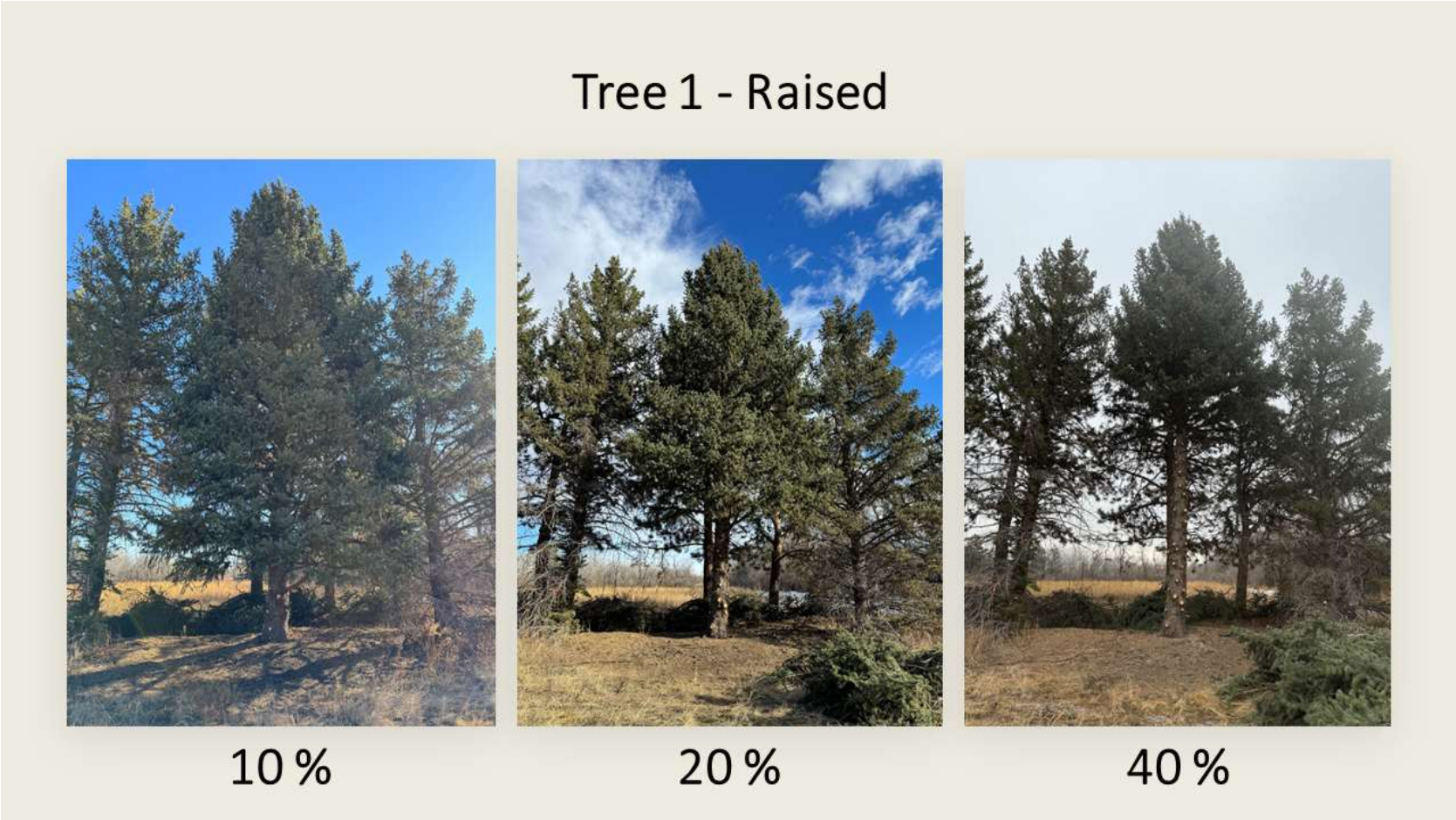

Figure 18 Photographs of Colorado blue spruce (*Picea pungens*) Tree 1 raised by 10%, 20%, and 40% (left to right).

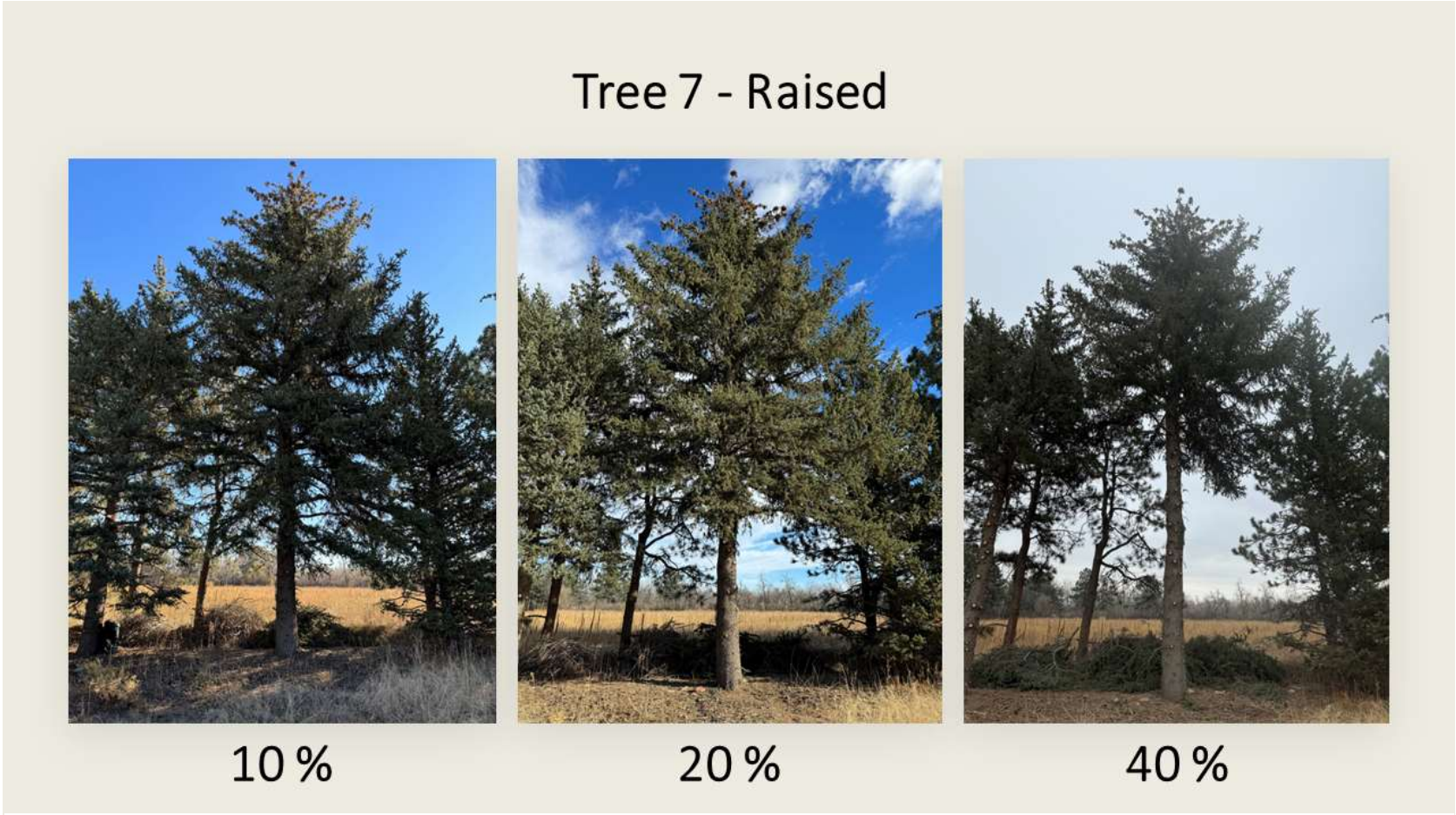

Figure 19 Photographs of Colorado blue spruce (*Picea pungens*) Tree 7 raised by 10%, 20%, and 40% (left to right).

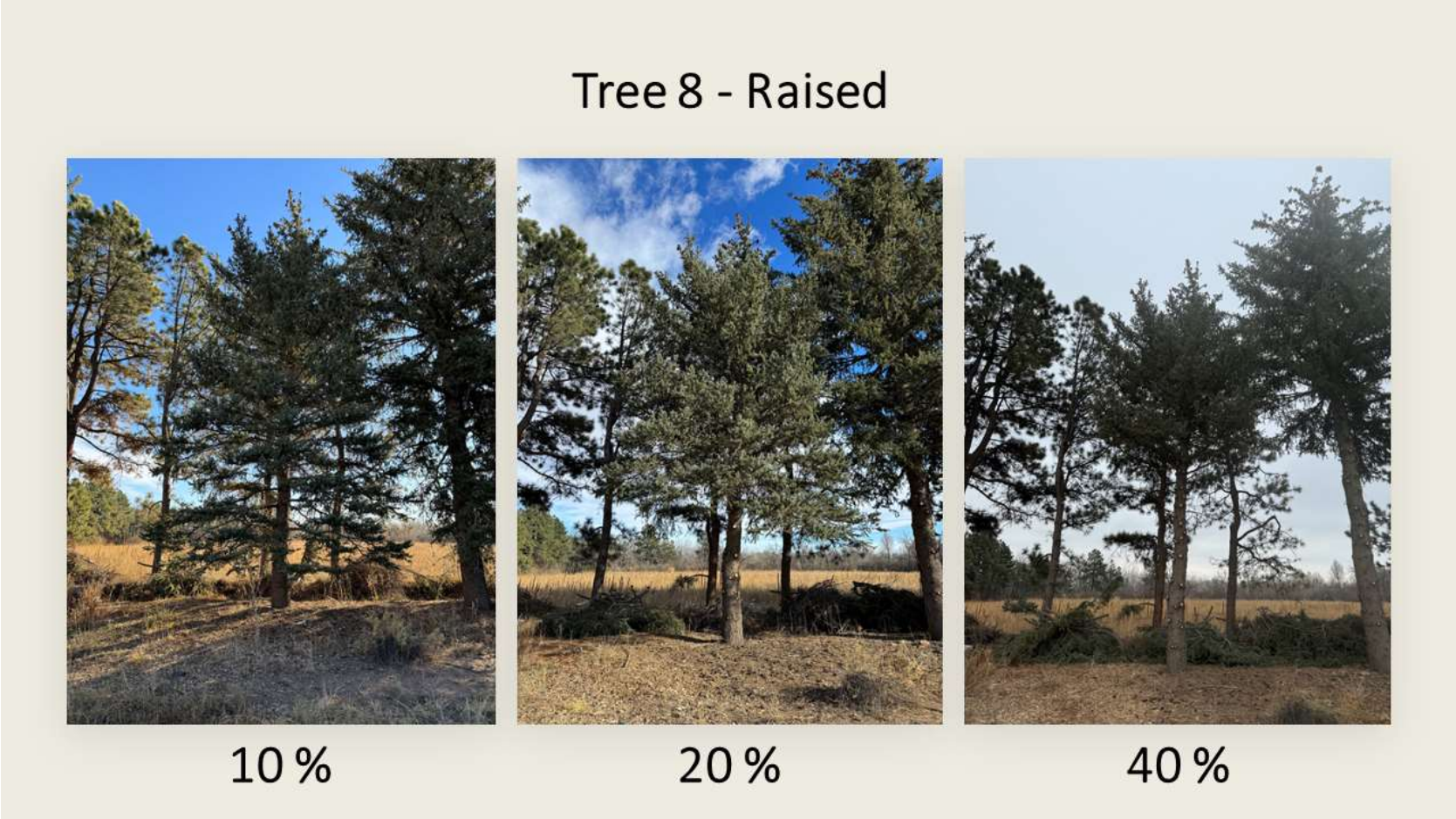

Figure 20 Photographs of Colorado blue spruce (*Picea pungens*) Tree 8 raised by 10%, 20%, and 40% (left to right).

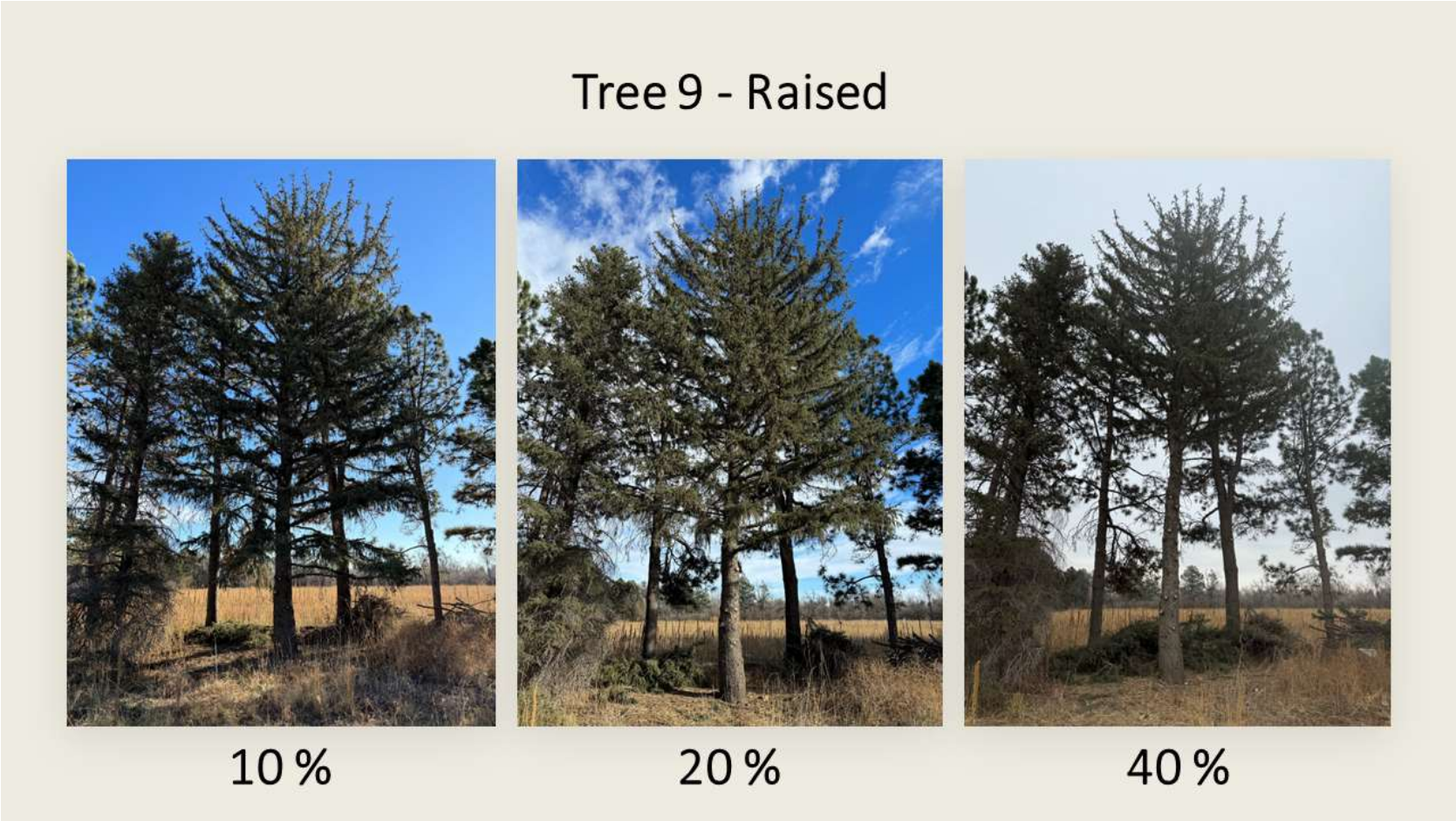

Figure 21 Photographs of Colorado blue spruce (*Picea pungens*) Tree 9 raised by 10%, 20%, and 40% (left to right).

APPENDIX B – THINNED TREATMENT ACCURACY TABLE & PHOTOGRAPHS

Table 5 Comparisons made between the target cumulative diameter (TCD) amounts and the actual cumulative diameter (ACD) to be removed from the top, middle, and bottom third of each tree canopy during the 10%, 20%, and 40% severity periods. The percent error is shown for respective thirds of each tree canopy (top, middle, and bottom) and total cumulative error for each tree at 10%, 20%, and 40% severity, respectively.

	Top			*Middle*			*Bottom*			
Subject	**TCD (mm)**	**ACD (mm)**	**Error (%)**	**TCD (mm)**	**ACD (mm)**	**Error (%)**	**TCD (mm)**	**ACD (mm)**	**Error (%)**	**Total Error (%)**
Tree 2										
10 %	290.5	288.2	0.8	145.3	146.2	0.64	145.3	148.3	2.09	0.28
20 %	290.5	291	0.16	145.3	145	-0.18	145.3	144	-0.87	-0.18
40 %	581.1	581.2	0.02	290.5	287.1	-1.18	290.5	303.4	4.43	0.82
Tree 3										
10 %	194.5	195.7	0.59	97.3	90.8	-6.65	97.3	97	-0.28	1.44
20 %	194.5	202.7	4.19	97.3	106.7	9.69	97.3	95.1	-2.23	3.96
40 %	389.1	388.3	-0.2	194.5	223.2	14.73	194.5	187.5	-3.62	2.68
Tree 4										
10 %	322.5	322.7	0.06	161.2	162.4	0.71	161.2	160	-0.77	0.02
20 %	322.5	323.8	0.4	161.2	183.5	13.8	161.2	154.1	-4.43	2.54
40 %	645	650	0.82	322.5	333	3.26	322.5	328.6	1.89	1.7
Tree 5										
10 %	310.4	309.1	-0.41	155.2	153.8	-0.9	155.2	154.5	-0.44	-0.54
20 %	310.4	310.4	0	155.2	169.9	9.48	155.2	160.3	3.29	3.2
40 %	620.8	618.7	-0.33	310.4	309.7	-0.22	310.4	311.9	0.49	-0.1
Tree 6										
10 %	261.5	265.4	1.49	130.8	130.3	-0.35	130.8	134.7	3.02	1.41
20 %	261.5	261.2	-0.12	130.8	128.3	-1.88	130.8	130.4	-0.27	-0.6
40 %	523	521.1	-0.37	261.5	263.8	0.87	261.5	261.7	0.07	0.05

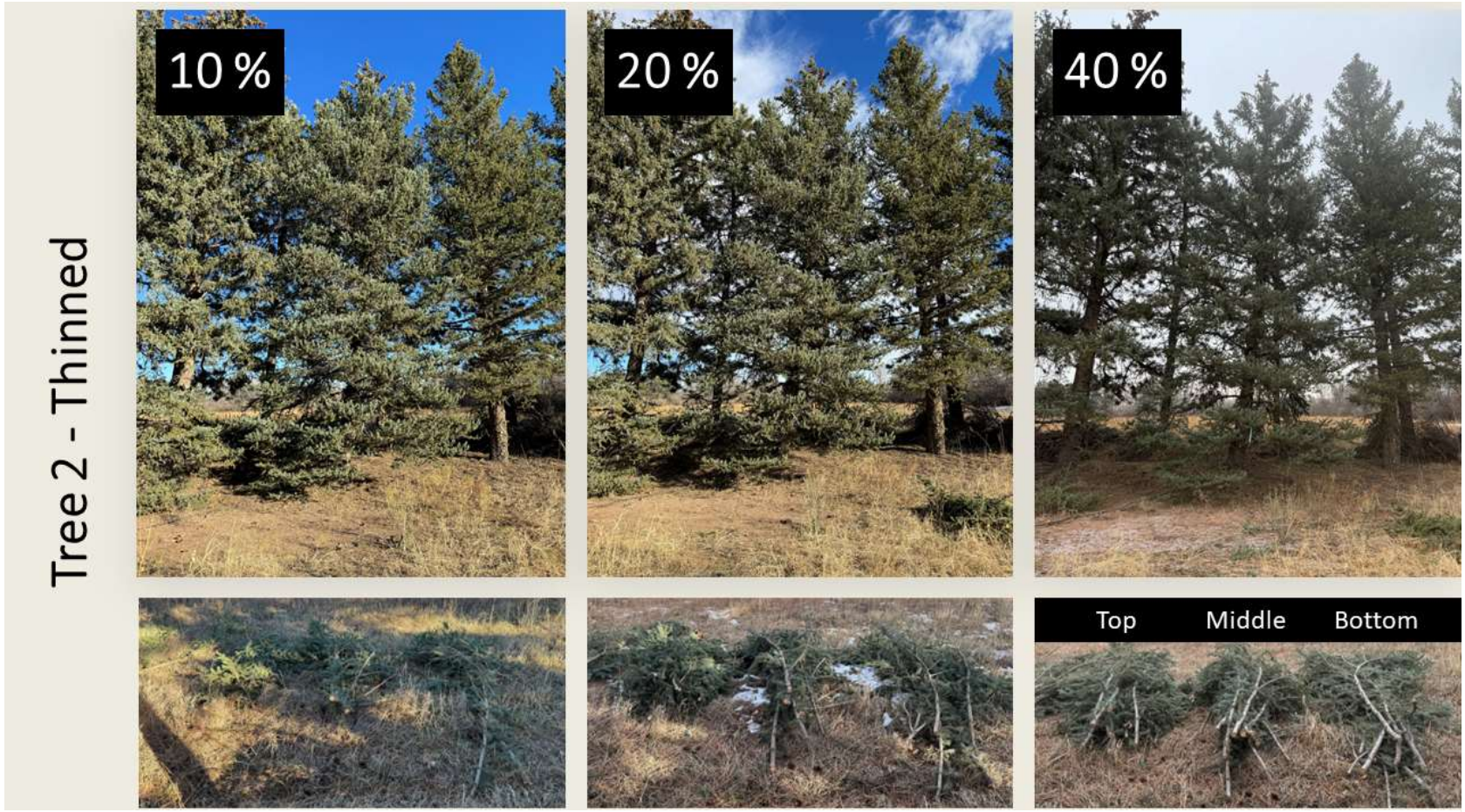

Figure 22 Photographs of Colorado blue spruce (*Picea pungens*) Tree 2 thinned by 10%, 20%, and 40% (left to right). Pictured below each severity is the corresponding cumulative material removed from the top, middle, and bottom thirds during each period (left to right).

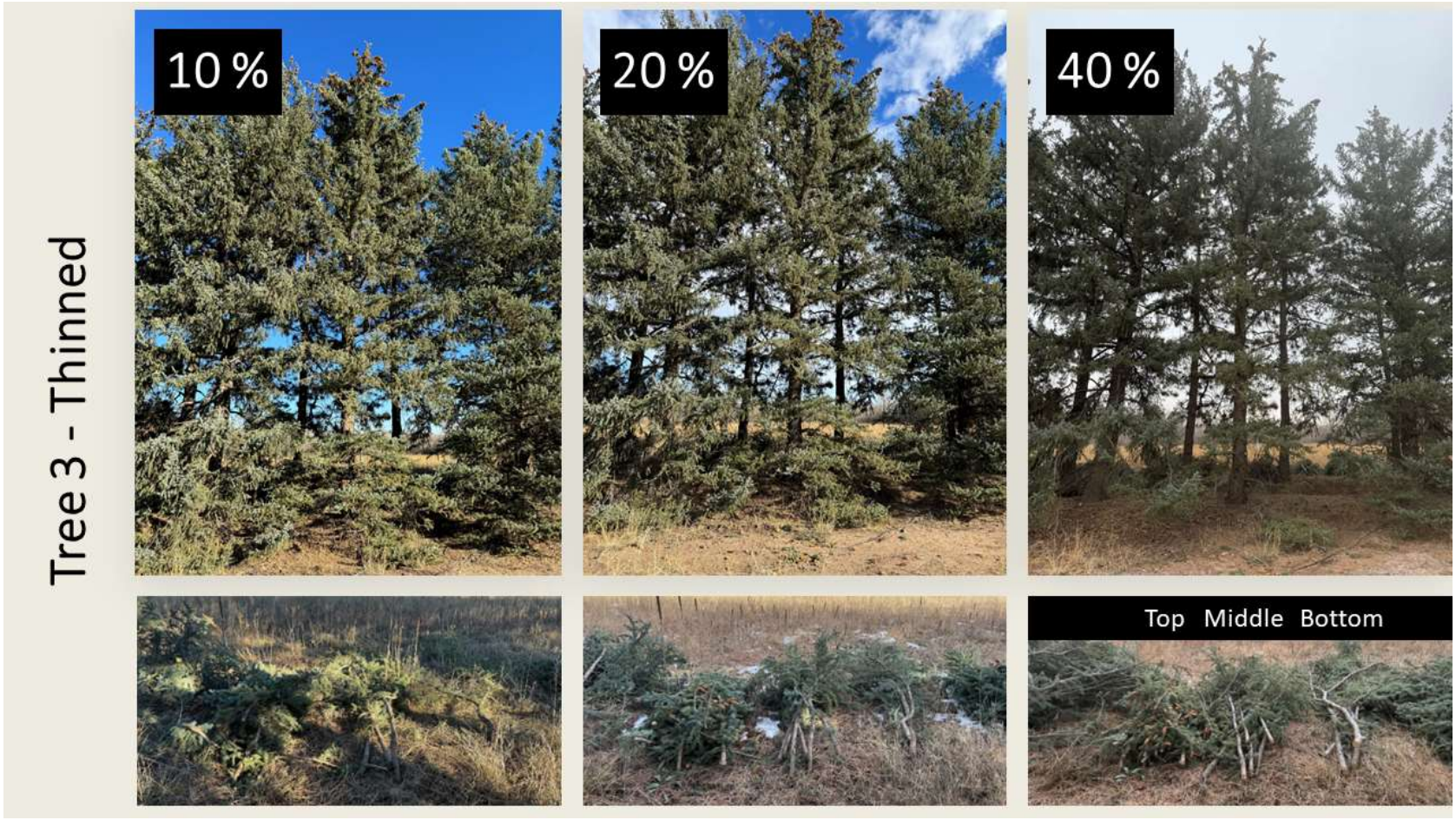

Figure 23 Photographs of Colorado blue spruce (*Picea pungens*) Tree 3 thinned by 10%, 20%, and 40% (left to right). Pictured below each severity is the corresponding cumulative material removed from the top, middle, and bottom thirds during each period (left to right).

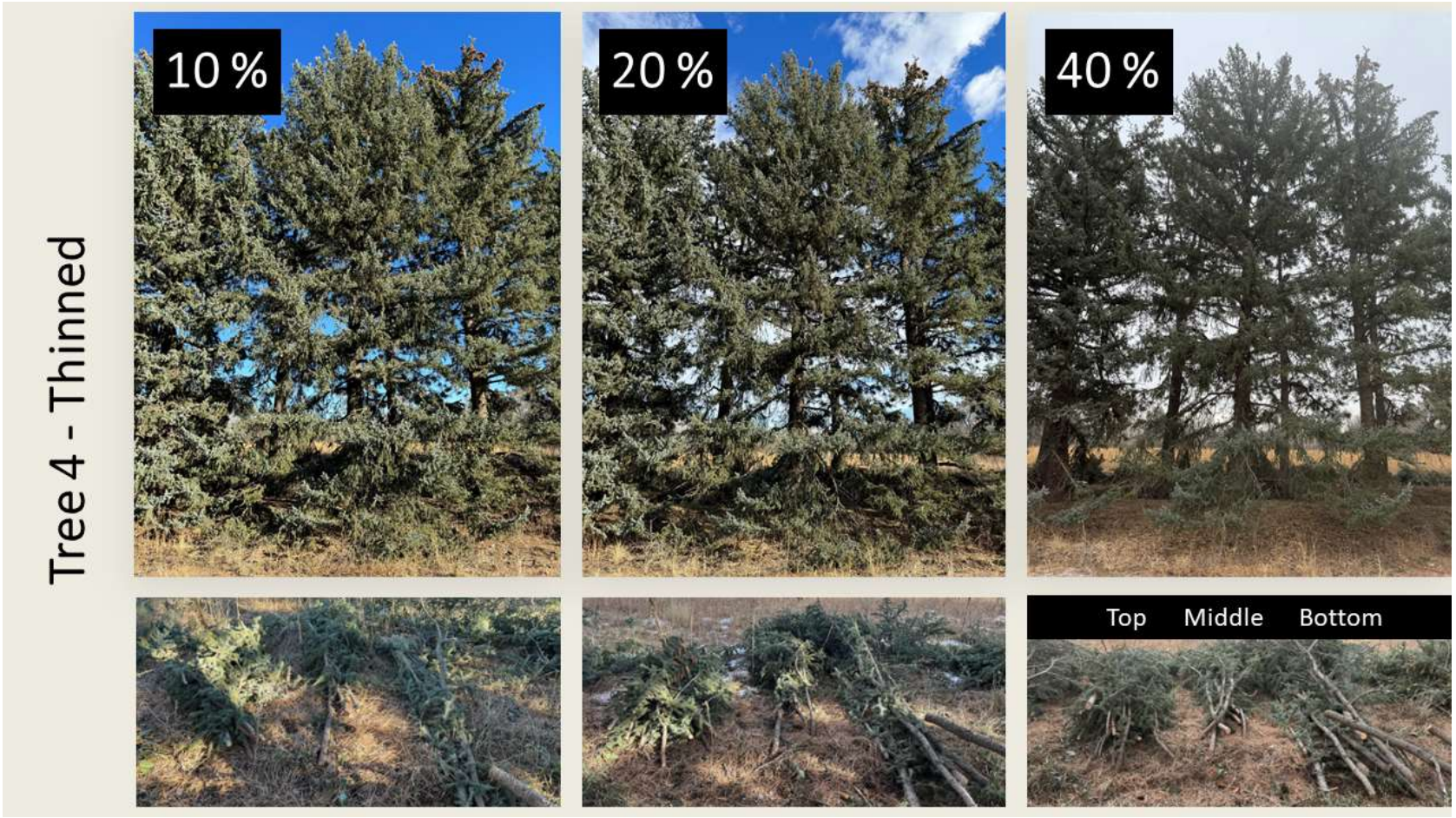

Figure 24 Photographs of Colorado blue spruce (*Picea pungens*) Tree 4 thinned by 10%, 20%, and 40% (left to right). Pictured below each severity is the corresponding cumulative material removed from the top, middle, and bottom thirds during each period (left to right).

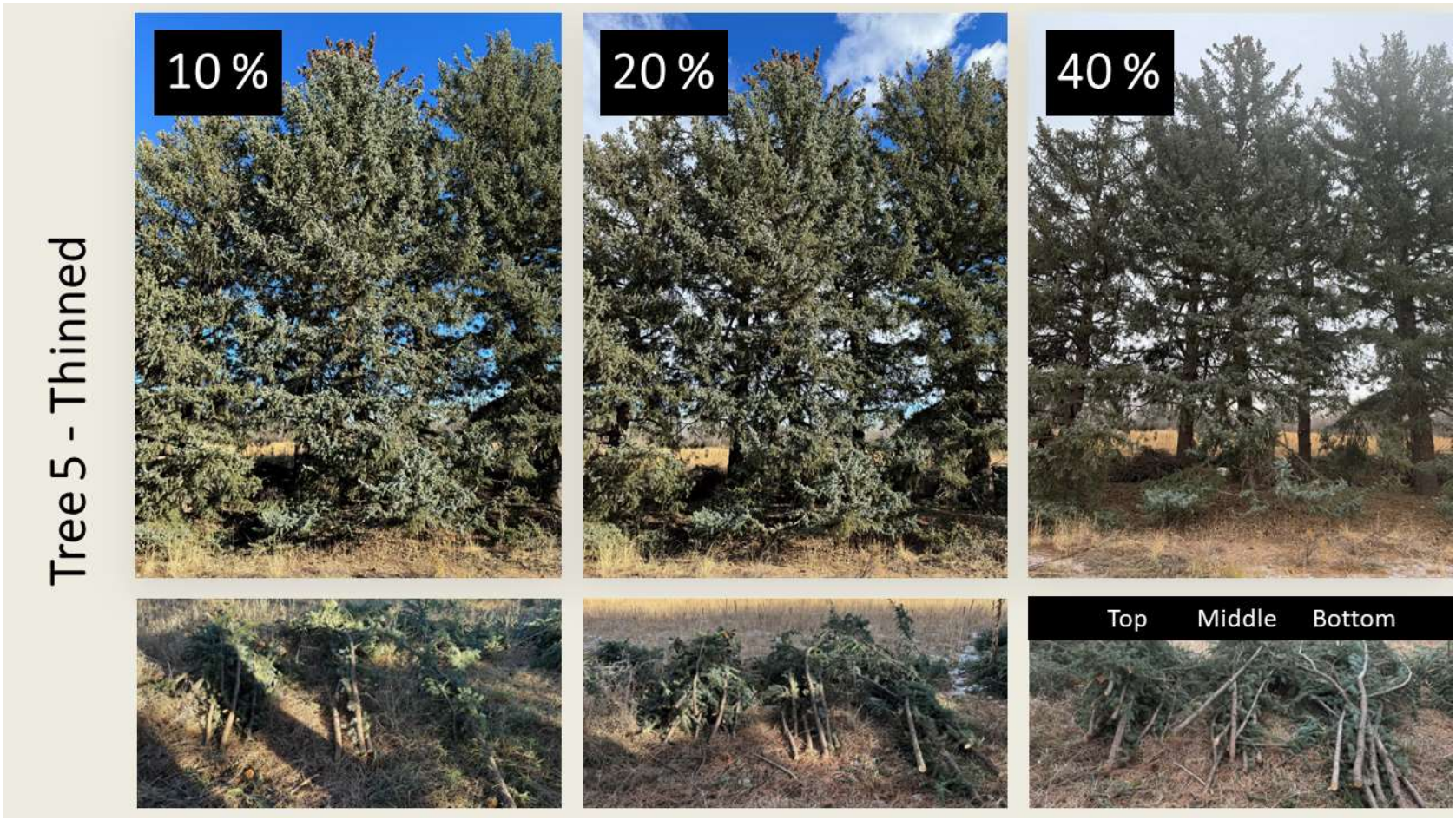

Figure 25 Photographs of Colorado blue spruce (*Picea pungens*) Tree 5 thinned by 10%, 20%, and 40% (left to right). Pictured below each severity is the corresponding cumulative material removed from the top, middle, and bottom thirds during each period (left to right).

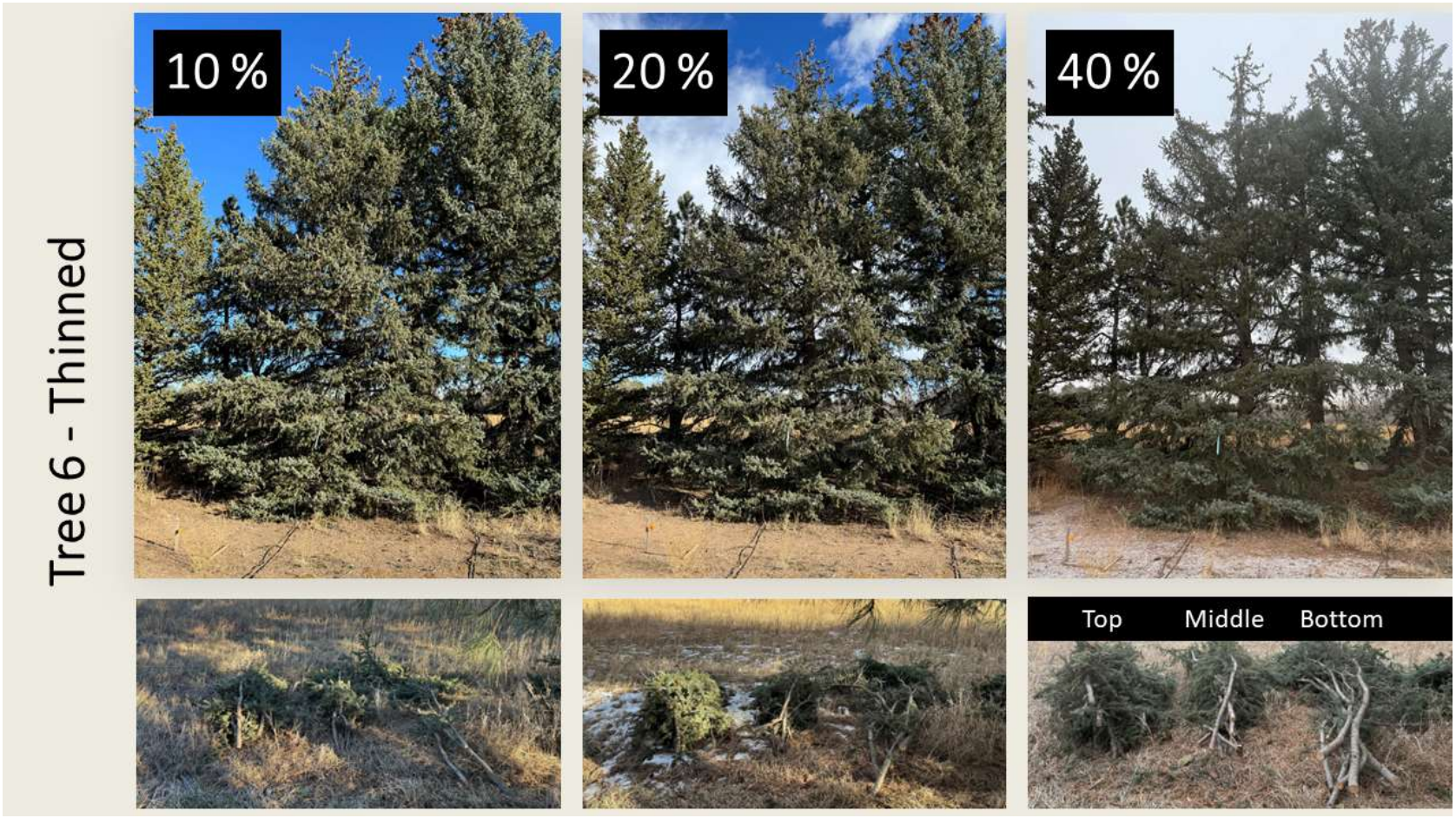

Figure 26 Photographs of Colorado blue spruce (*Picea pungens*) Tree 6 thinned by 10%, 20%, and 40% (left to right). Pictured below each severity is the corresponding cumulative material removed from the top, middle, and bottom thirds during each period (left to right).

APPENDIX C – INDIVIDUAL SCATTER PLOTS SHOWING RELATIONSHIP OF 30-MINUTE MAXIMUM WIND SPEEDS AND 30-MINUTE MAXIMUM BENDING MOMENTS BY SEVERITY

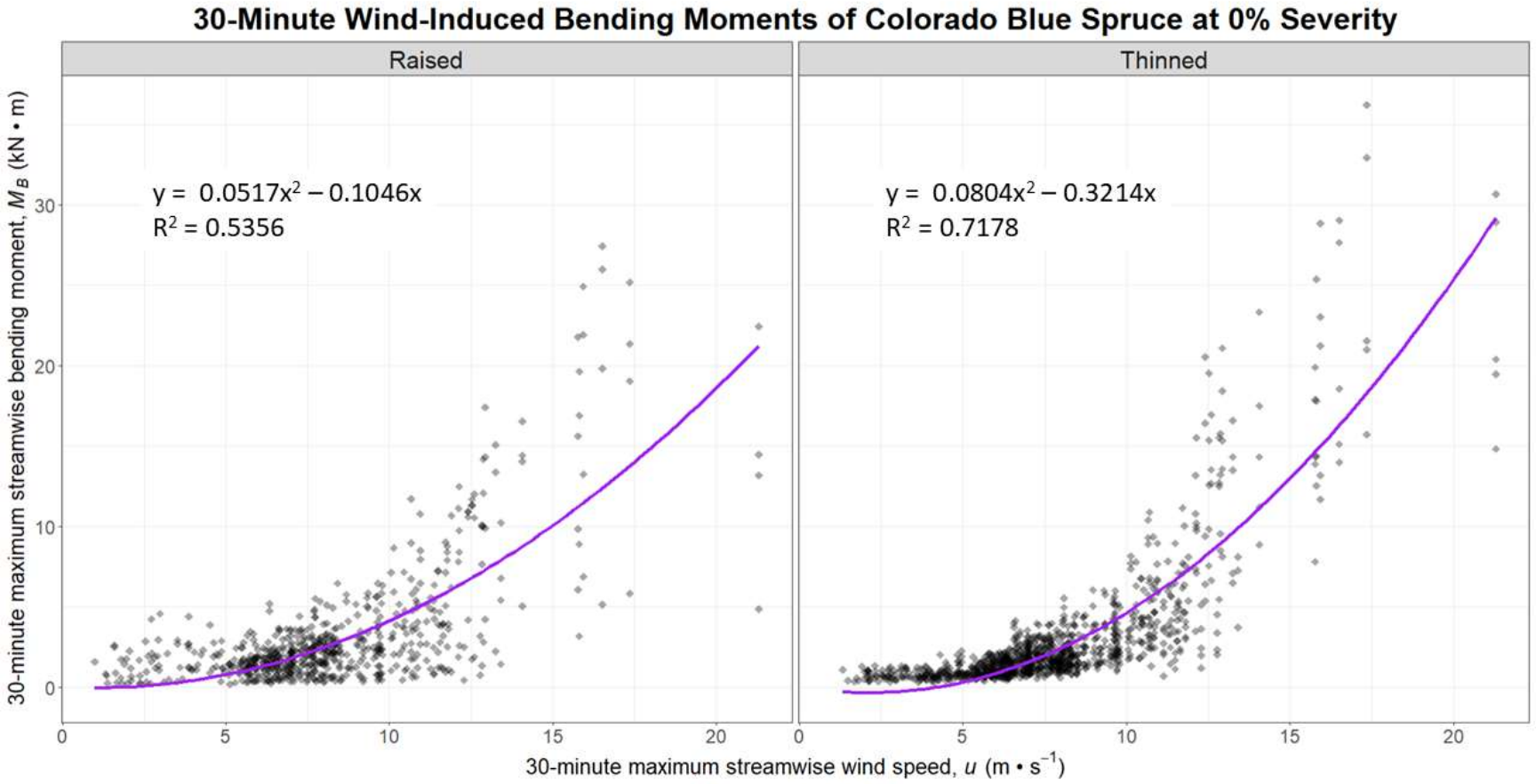

Figure 27 Split plot showing the positive quadratic relationship between 30-minute maximum wind speed and 30-minute maximum bending moments for all raised trees (left plot) and thinned trees (right plot) during the 0% severity period. Darker areas indicate increased density of data points at that wind speed and resulting bending moment.

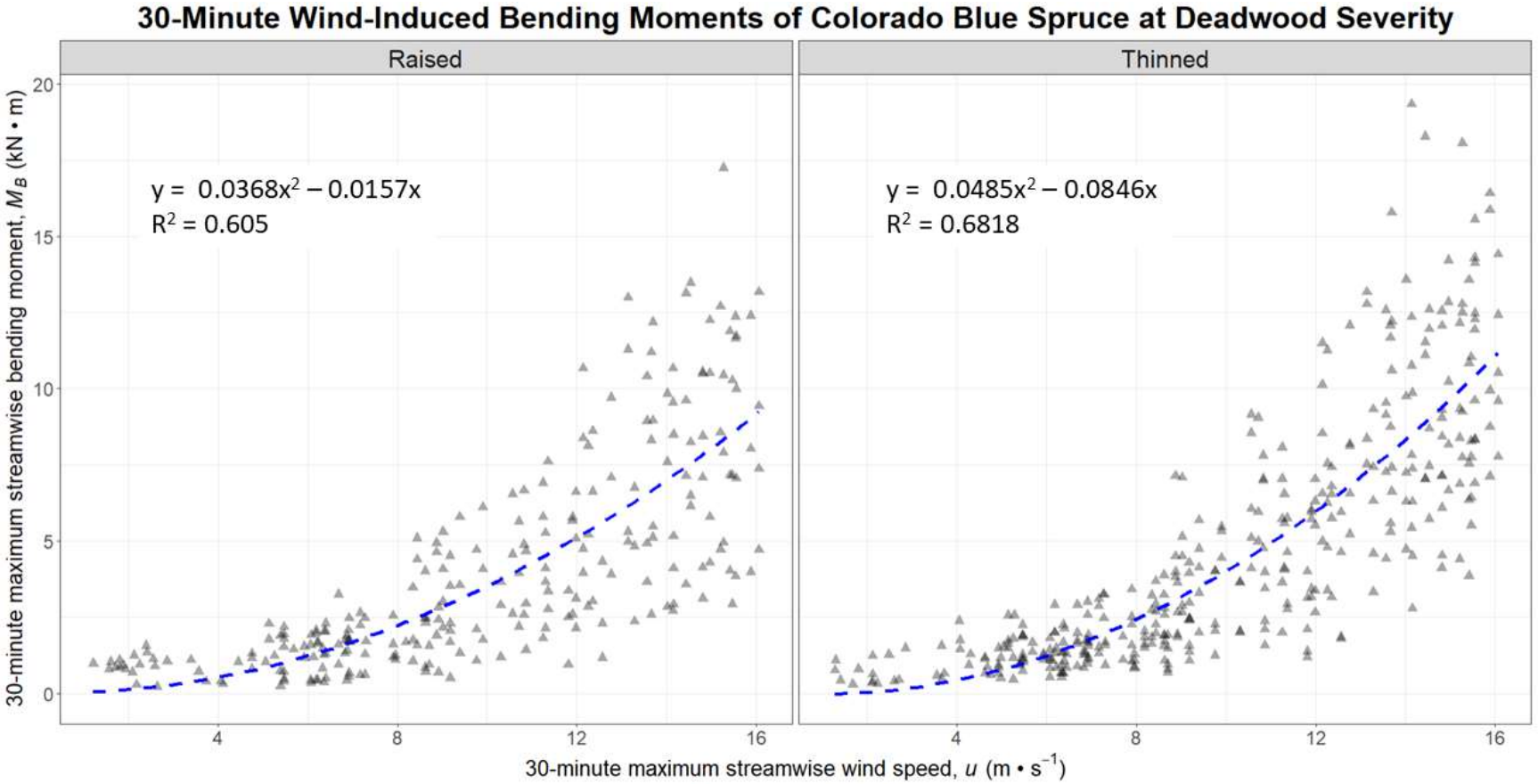

Figure 28 Split plot showing the positive quadratic relationship between 30-minute maximum wind speed and 30-minute maximum bending moments for all raised trees (left plot) and thinned trees (right plot) during the deadwood severity period. Darker areas indicate increased density of data points at that wind speed and resulting bending moment.

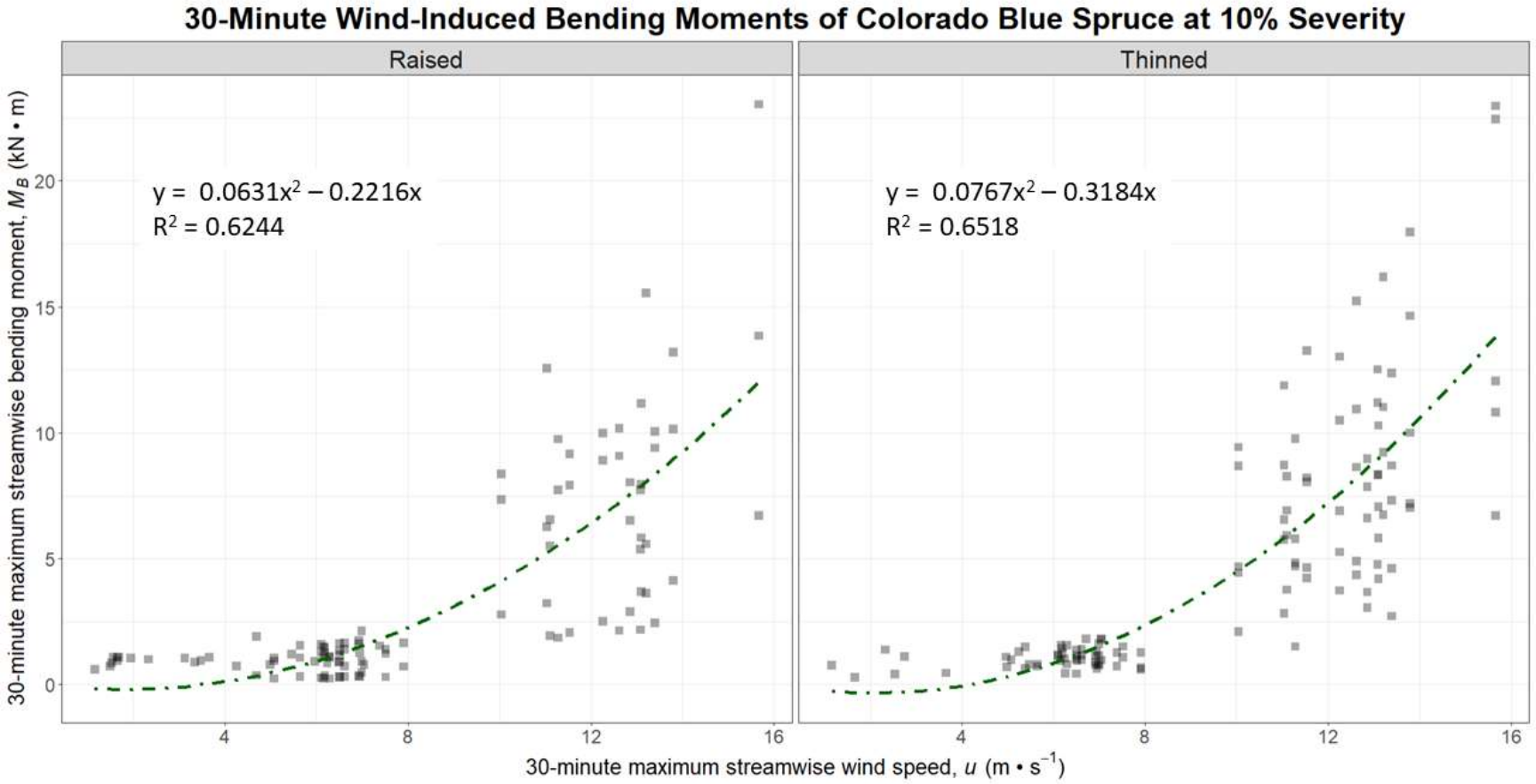

Figure 29 Split plot showing the positive quadratic relationship between 30-minute maximum wind speed and 30-minute maximum bending moments for all raised trees (left plot) and thinned trees (right plot) during the 10% severity period. Darker areas indicate increased density of data points at that wind speed and resulting bending moment.

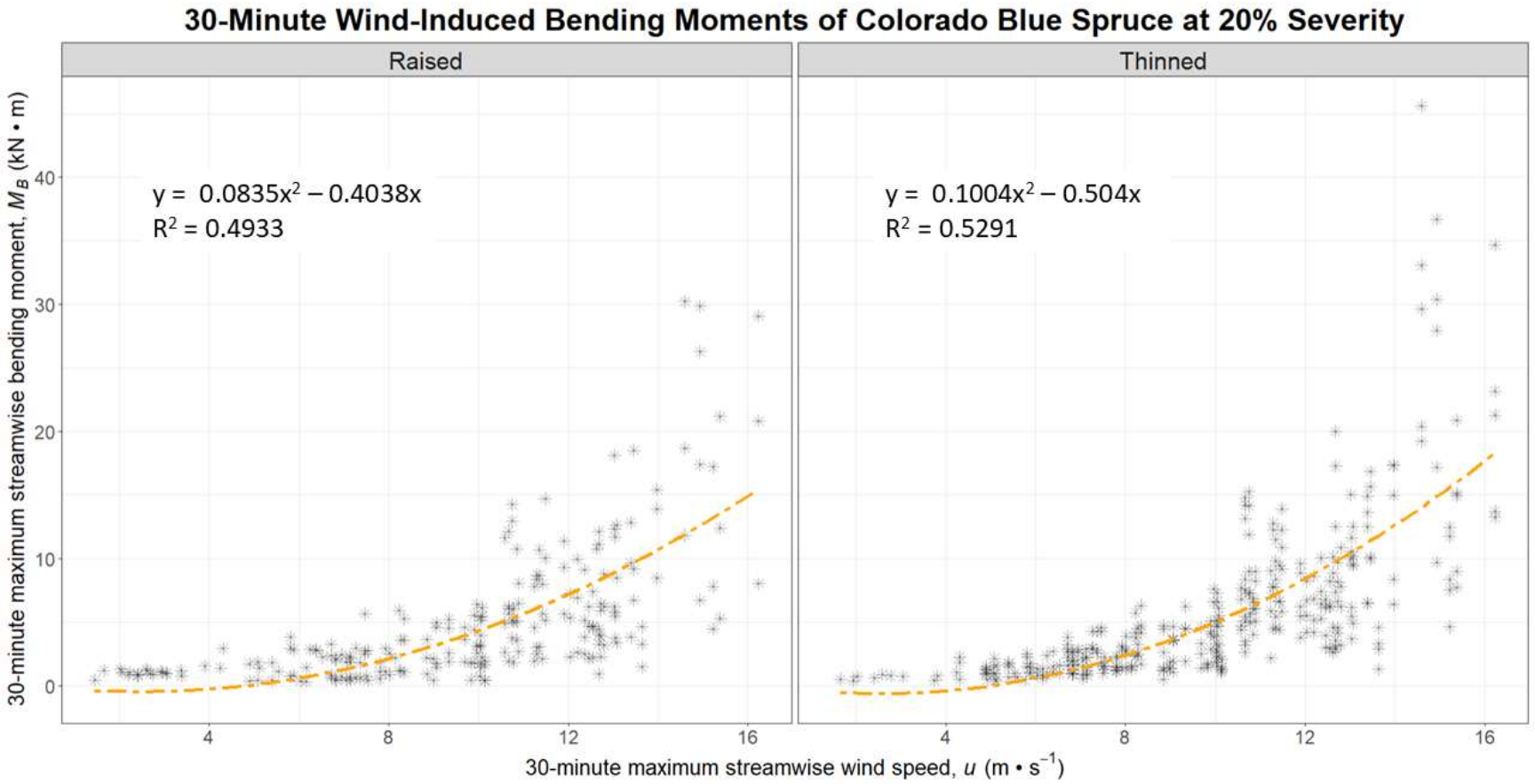

Figure 30 Split plot showing the positive quadratic relationship between 30-minute maximum wind speed and 30-minute maximum bending moments for all raised trees (left plot) and thinned trees (right plot) during the 20% severity period. Darker areas indicate increased density of data points at that wind speed and resulting bending moment.

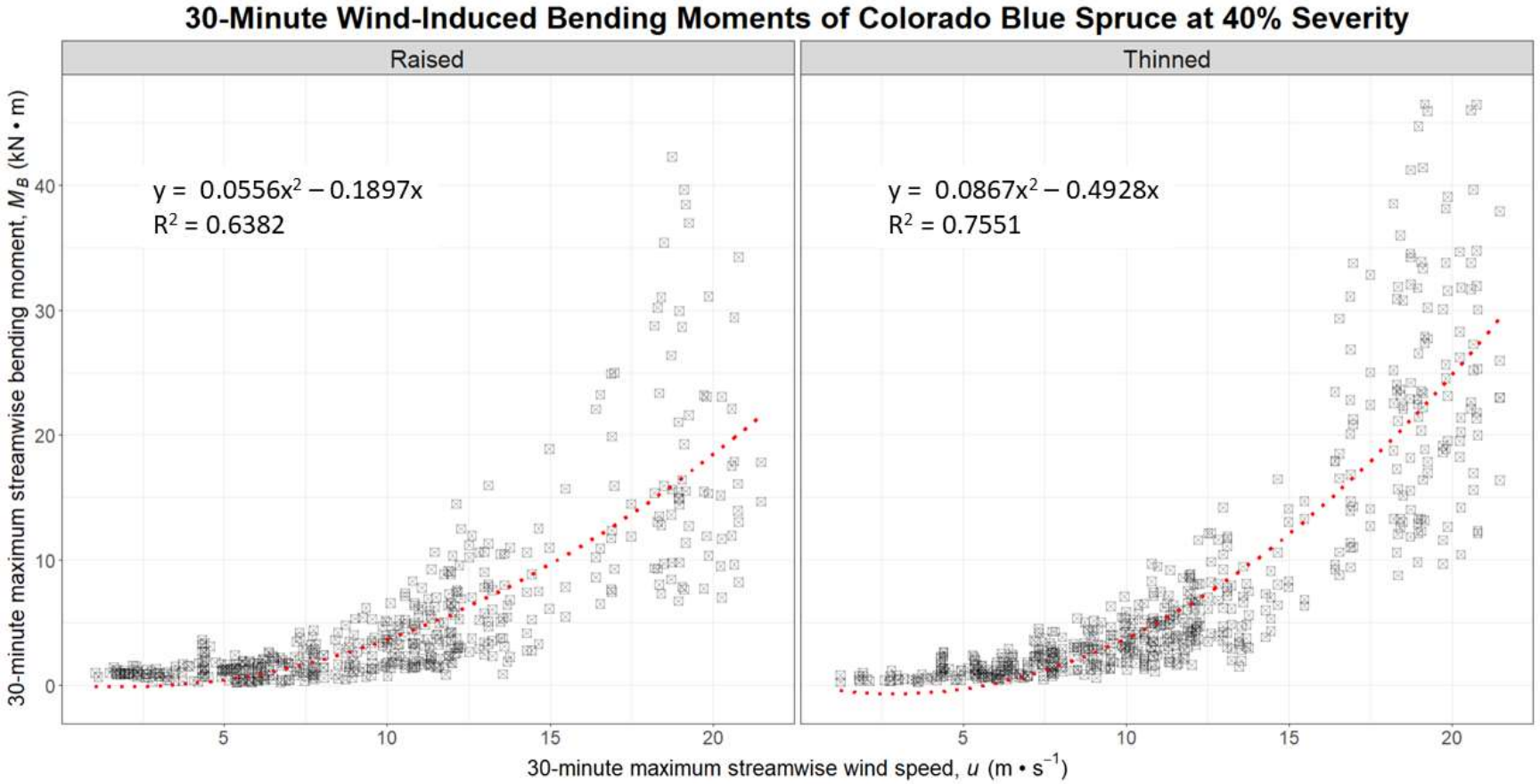

Figure 31 Split plot showing the positive quadratic relationship between 30-minute maximum wind speed and 30-minute maximum bending moments for all raised trees (left plot) and thinned trees (right plot) during the 40% severity period. Darker areas indicate increased density of data points at that wind speed and resulting bending moment.